Environmental Earth Sciences (2022) 81:13
https://doi.org/10.1007/s12665-021-10066-1

THEMATIC ISSUE

Consolidation of volcanic tuffs with TEOS and TMOS: a systematic study

Christopher Pötzl[1] · Stine Rucker[1] · Eberhard Wendler[2] · Siegfried Siegesmund[1]

Received: 24 March 2021 / Accepted: 11 October 2021 / Published online: 8 December 2021

Abstract
In this study, nine volcanic tuffs from Armenia, Germany and Mexico were treated with two commercially available consolidants on base of silicic acid ester, as well as different pretreatments with an anti-swelling agent and/or primer components. Prior to the treatment, the tuffs were analyzed regarding their petrography and mineralogy, with a greater focus on their clay mineral content. The effect of the consolidation was evaluated by comparative analyses of petrophysical properties and weathering behavior before and after the treatments. The main goals of this study were to identify a general suitability of different consolidating treatments for different types of tuff, evaluating tartaric acid as a primer component for tuff consolidation and to pursue the approach of finding a molecular answer for apparent tuff consolidation problematics, by testing a consolidation agent with smaller molecule sizes than current products on the market: tetramethoxysilane (TMOS).

Keywords Consolidation · TEOS · TMOS · Volcanic tuff · Building stones

Introduction

Volcanic tuff is a widespread material used in countless heritage monuments worldwide (Fig. 1) and considered a problematic stone when it comes to conservation measures. Compared to other popular heritage building stones like marble, sandstone or granite, tuffs usually show higher sensitivity to weathering. The reasons are manifold and often traced back to their diverse depositional environments that cause a strong mineralogical and fabric heterogeneity (Auras and Steindlberger 2005; Steindlberger 2020). The heterogeneous character of the tuffs leads to a wide range of properties and weathering behavior. Increased porosity and capability for water absorption, together with an overall low strength and a frequent occurrence of swelling clays, leading to additional stress due to expansional processes, result in a reduced durability of the material and ultimately to pronounced forms of deterioration (Pötzl et al. 2018a). The deterioration leads to a reduction of strength, progressing from the surface into the core of the stone. Stone consolidation therefore aims to equalize this strength discrepancy and to restore a uniform strength profile, comparable to the sound, unweathered rock (Snethlage and Sterflinger 2011).

Satisfactory consolidation of volcanic tuffs has shown to be a challenging task. Due to their high porosities and unfavorable pore size distributions, as well as their partly high content of swelling clays, there are several criteria for a successful consolidation of volcanic tuffs. Standardized techniques applied on tuffs do often not lead to satisfying results. Instead, special procedures with formulations adjusted to the individual case have to be developed, which is a time consuming and costly endeavor (Wendler et al. 1996; Wendler 2005; Steindlberger 2020).

One reason for the reduced penetration ability of the consolidant can be the blocking of the pore entrance of small pores due to present pore water. Some tuffs have the ability to absorb considerable amounts of water from the air at low relative humidity levels (Yasar 2020). This water can be retained by micropores for a considerable amount of time. The ability to store water may be additionally increased by

This article is part of a Topical Collection in Environmental Earth Sciences on "Building Stones and Geomaterials through History and Environments – from Quarry to Heritage. Insights of the Conditioning Factors", guest edited by Siegfried Siegesmund, Luís Manuel Oliveira Sousa, and Rubén Alfonso López-Doncel.

✉ Christopher Pötzl
christopher.poetzl@gmx.de

[1] Geoscience Centre of the University Goettingen, Goettingen, Germany

[2] Fachlabor für Konservierungsfragen in der Denkmalpflege, Munich, Germany

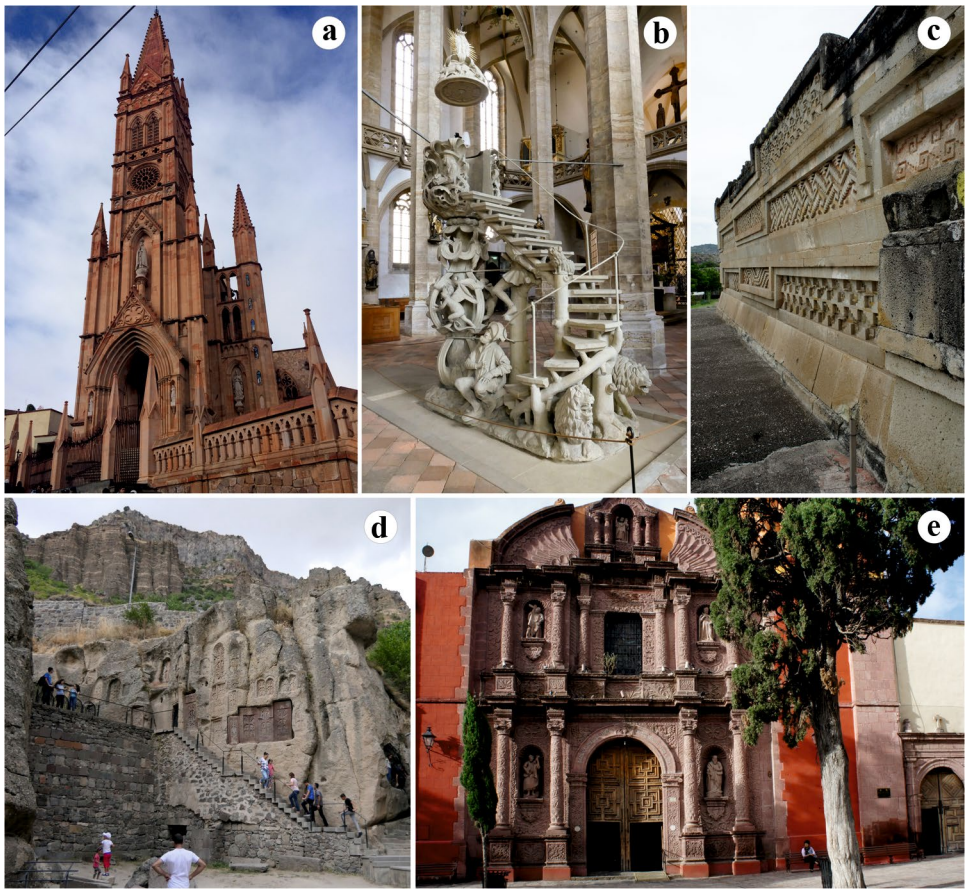

Fig. 1 Application of different tuff varieties in architectural heritage around the globe. **a** Nineteenth century Templo de Fatima in Zacatecas, Mexico; **b** sixteenth century Tulip Pulpit in the Freiberg Cathedral, Germany; **c** second century Mitla pyramids, Mexico; **d** Cross stones at the fourth century Geghard monastery, Armenia; **e** Richly ornamented facade of the eighteenth century Templo de Nuestra Señora de la Salud in San Miguel de Allende, Mexico

the presence of clay minerals and zeolites. If, for example a bottleneck passage is filled with water, this water will block the consolidant from migrating further into the pore network of the stone (Wendler 2005, 2016). If the migration of the consolidant comes to a halt in this location, a part of the water in the bottleneck will be used for the hydrolysis of the consolidant and the bottleneck will be sealed irreversibly. This effect not only has a negative influence on the attempted conservation measure, but also complicates any future treatment.

Another limiting factor to overcome the problem of small pore entries is the molecular size of the consolidant itself. Many commercial consolidation products contain oligomeric molecule complexes that are too big to penetrate through pore entries that are in the nanometer scale. Highly sophisticated formulations of monomeric stone consolidants, like KSE300 from Remmers company, contain monomeric molecules as small as 1–1.5 nm. This size tends to be sufficiently small to penetrate the pore network of the majority of stone materials. However, some tuffs can contain micropores even smaller than 1 nm (Pötzl et al. 2018b). Especially micropores caused by zeolites, which are abundant in many tuffs, are usually smaller than 2 nm and frequently show ultramicropores < 0.7 nm (Korkuna et al. 2006). Even small amounts of these pores can lead to a sealing of bottlenecks and an inhibition of further migration of the consolidant (Wendler 2016).

A further reduction of the molecular size of the consolidants is possible, but only to a certain degree, as the ethoxy group is already the second simplest existing group out of the alcoxy groups. A downsizing may be reached by an exchange of the already simple ethoxy groups in the molecules of the silicic acid ester, by the simplest (and smaller) methoxy groups.

Bonding agents (primer) increase the chemical attraction for the consolidant and help the cross-linking of the silica gel with the substrate. The primer is inserted into the stone prior to the consolidation treatment and is meant to coat the pore walls. Because the mineral surface of calcite possesses few hydroxyl groups to which the consolidant can link, this kind of bonding assistance is frequently used for limestones and marble, to secure a better bonding between the consolidant and the substrate (Wheeler et al. 2000; Steinhäußer and Wendler 2004). Although siliceous stones possess more hydroxyl groups for the bonding of the consolidant, Wendler (2005) tested five potential primer components on tuffs, in order to investigate their effect on the efficiency of diluted consolidation products.

Tartaric acid was identified to increase the efficiency of the consolidation most effectively, without showing any drawbacks due to the application. Based on these results, tartaric acid was chosen as a primer component for this study.

Finally, the inhibition of moisture expansion in tuffs is frequently a further demand, to minimize the future damage potential within the stones' fabric. The expansion that is mostly controlled by the swelling and shrinking of clay minerals can be reduced by an anti-swelling agent. The anti-swelling agent enters the interlayer of swelling clays and replaces the exchangeable cations, that previously allowed the accumulation of additional water molecules that lead to a swelling process (Wendler et al. 1991). A full inhibition of the expansion is not possible, but the amount of expansion may be significantly reduced.

Materials and methods

Selected tuffs

Nine volcanic tuffs that are used as building stones in Armenia, Germany and Mexico were selected: three (comparably) low porous tuffs labelled as Blanca Pachuca (BP), Blue Sevan (BS) and Loseros (LOS), as well as six moderately to highly porous tuffs Noyemberyan (NB), Cantera Verde (CV), Cantera Rosa (CR), Hoktemberyan Red (HR), Weibern (WB) and San Miguel el Alto (SMA) (in ascending order). Sample specimens of all nine tuffs were prepared as follows and subjected to the same treatment:

- cubes of 65 mm edge length, for porosity, density and water absorption measurements
- cylindric samples of 40 mm height and diameter in *X* and *Z* direction (*X* = parallel, *Z* = perpendicular to the bedding), which were later cut into 10 mm discs to measure the water vapor diffusion resistance
- cylindric samples of 50 mm height and 15 mm diameter in *X* and *Z* direction, for ultrasonic velocity, hydric, thermal and thermo-hydric expansion measurements

The selection of tuffs was based on preliminary analyses of petrographical and petrophysical properties. The goal was to evaluate the different consolidation treatments for a wide range of tuffs with highly varying mineralogy and other properties. The fraction of micropores < 0.1 µm and the hygroscopic water sorption behavior were especially decisive, to identify potential problems with differential water absorption capabilities of the tuffs. Another decisive reason was the abundance (or absence) of swelling clays that increase hydric expansion. Therefore, most of the selected tuffs show considerable amounts of swelling clays and/or an abundance of zeolites.

Conservation materials and application

Two silicic acid esters were selected for the consolidation. The selection of the consolidants based on their molecular size (< 2 nm). As described above, micropores that show small pore entrance radii may limit the intake of the consolidant and therefore molecular sizes should be as small as possible.

The first consolidant, KSE 300 from Remmers, is based on ethyl silicate (tetraethoxysilane TEOS) and frequently used in stone conservation. The commercially available KSE 300 (for the rest of this study labeled as TEOS or KSE) is a single-component system with a gel deposition rate of approximately 30% and characterized by mainly monomeric molecules of 1–1.5 nm size. However, the formulation of KSE300 can contain up to octamers. Since 2010, the formulation of KSE 300 from Remmers does not longer contain organostannic compounds as catalysts. The currently applied catalyst is company secret (verbal communication from J. Engel (Remmers) 2020).

The second consolidant is a silicic acid ester based on methyl silicate (tetramethoxysilane TMOS) which was used as stone consolidant in the 60s and 70s, before it was withdrawn from the market for its toxicity (Snethlage and Sterflinger 2011). Scherer and Wheeler (2008) point out that of the methoxysilanes that may be used as consolidants, 99% of the time methyltrimethoxysilane (MTMOS) was applied under the commercial name BRETHANE, rather than TMOS. Main health hazards are the release of methanol during hydrolysis reaction, affecting the eyes and respiratory tract during application (GESTIS Substance Database, https://gestis.dguv.de/data?name=106781&lang=en, Accessed 20 Mar 2021). The indoor critical value in the air is 250 ppm, which may be reached easily by an indoor conservation measure. However, outdoor application normally should not have severe consequences. Note that methanol is also called wood spirit, since it is evolved from heated wood, thus one is exposed to it even during sitting around a campfire. The fully cured silica gel, however, is not harmful. TMOS is characterized by monomeric molecules, low viscosity and high reactivity. The methoxy groups bound to the silicon atom in a TMOS molecule are smaller than the ethoxy groups in a TEOS molecule, so that TMOS provides a smaller overall molecular size (< 1 nm). In this study TMOS was applied uncatalyzed as a neat monomer.

Following the approach of Wendler (2005), the samples were impregnated with either of the two consolidants on base of ethyl silicate (TEOS ≙ KSE 300 from Remmers) or methyl silicate (TMOS from Acros Organics) as well as in

combination with a primer component (tartaric acid $C_4H_6O_4$ from Merck) and/or an anti-swelling agent (Antihygro from Remmers). The tartaric acid (labelled as WS for the rest of the study) obtained from Merck was used as a primer component and is meant to line the walls of the pores and enhance the bonding with the consolidant (Wheeler et al. 2000). By increasing the attraction for the consolidant, the efficiency of the absorption, penetration depth and bonding to the substrate is expected to be increased. The anti-swelling agent (Antihygro) obtained from Remmers (aqueous solution of 1,4-diaminobutane dihydrochloride) is meant to enter the interlayer of swelling clays and replace the exchangeable cations (Wendler et al. 1991). The cation exchange ensures a reduced swelling of the stone due to a reduced potential of water accumulation in the interlayer of the clay minerals. However, the Antihygro is an additional chemical that has an impact on the materials petrophysics and should only be applied after adequate laboratory testing (Snethlage and Pfanner 2020). Following this recommendation, the anti-swelling agent was additionally applied to tuffs that lack swelling clays or do not show considerable expansional behavior, in order to identify potential drawbacks. The Antihygro (A) was always applied prior to the consolidation and the primer.

To evaluate the impact of all the above mentioned components, nine different combinations of treatment were conducted (see Fig. 2): (1) Exclusive treatment with the anti-swelling agent. (2) Exclusive treatment with the consolidant TEOS (KSE) or (3) TMOS. (4) Anti-swelling agent (A) in combination with TEOS (A + KSE) or (5) with TMOS (A + TMOS). (6) Tartaric acid with TEOS (WS + KSE) or (7) TMOS (WS + TMOS). (8) Anti-swelling agent in combination with tartaric acid and TEOS (A + WS + KSE) or (9) with TMOS (A + WS + TMOS). For all combinations, the petrophysical properties and weathering behavior of the rocks were analyzed before and after the treatments, in accordance to the European standards parallel (*X* direction) and perpendicular (*Z* direction) to the bedding.

The Antihygro and tartaric acid (0.3%) were applied to oven dried samples (40 °C) after an equilibration time of 60 min to room temperature. The samples were placed in a plastic tub and absorbed the chemicals by capillary forces for around 30 min before they were fully immersed for 1 h. After the Antihygro treatment, the samples were dried for several days and subsequently treated with either tartaric acid or a consolidant (consolidation only after being preconditioned). The fully saturated samples treated with tartaric acid were left at room conditions (~ 23 °C and 50% relative humidity) for 24 h (40 × 40 mm cylinders for 48 h, 65 × 65 mm cubes for 72 h) before they were treated with the consolidant. In this way the moisture content of the specimens should be approximated to the preconditioned samples from the climate chamber (23 °C/70% RH). Untreated specimens and specimens treated with Antihygro were preconditioned in a climate chamber at 23 °C and 75% relative humidity for at least 1 week, before being treated with the consolidant.

For the consolidation treatment, the specimens were placed in a solvent resistant plastic tub and first capillary absorbed the solutions for about 20 min under continuous refill of the consolidant, until the samples were fully covered. The samples were left under full immersion for 4–6 h to ensure full saturation. After the application of the consolidants, the samples were subsequently stored in a 23 °C/60% relative humidity climate for 6 weeks, until full curing of the consolidants. For TMOS consolidated samples, the storage conditions were adjusted to 85% relative humidity, since it evaporated too quickly when taken out of the consolidation bath and stored at 60% RH. After 6 weeks of curing, the samples were dried to constant mass (40 °C) and subsequently analyzed.

It should be noted that this work has to be seen as a pure laboratory (efficacy) study. The goal was to determine if and how different combinations of conservation materials influence the petrophysical properties of different types of tuffs and to identify whether or not certain treatments may ensure an enhancement of the rock properties. To exclude that any extrinsic factors affect the results of the consolidation treatment, all samples were fully saturated. The consolidants were applied on fresh quarry material, so the conditions for every combination of treatments were roughly the same. However, the partly strong heterogeneity of the individual tuff specimens needs to be taken into account. Especially in the lapilli tuffs, large pumice clasts

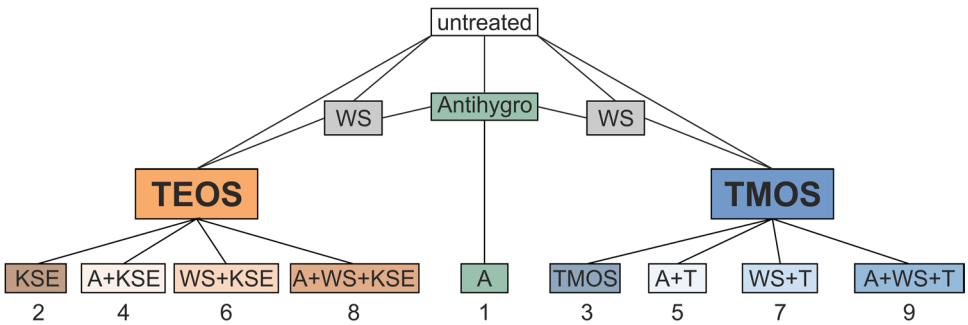

Fig. 2 Flowchart of the 9 conducted combinational consolidation treatments (bottom row). A = Antihygro (anti-swelling agent); WS = tartaric acid (primer); KSE = TEOS; T = TMOS

within the specimens for example may affect the water absorption and other petrophysical properties.

Analyses of the petrography and technical parameters

The petrographical analyses of each sample were performed on oriented thin sections under a polarisation microscope, as well as on a scanning electron microscope (SEM) with attached energy dispersive X-ray spectroscopy (EDX) for mineral identification. X-ray diffraction (XRD) of whole rock samples and oriented slides of the clay fraction < 2 µm along with X-ray fluorescence (XRF) were used for the mineralogical and geochemical characterization. They were supported by analysis of the cation-exchange capacity (CEC) analyses determined after the copper (II) triethylenetetramine method of Dohrmann and Kaufhold (2009), modified from Meier and Kahr (1999).

The effective porosity, bulk and matrix densities were determined by hydrostatic weighing of sample cubes of 65 mm edge length after DIN 772-4. The quotient of unforced (atmospheric conditions) and forced (vacuum) water saturation was used to determine the saturation degree S (Hirschwald 1912). The pore radii—or more correct—the pore throat radii distribution of the samples was determined on sample fragments after DIN66133 by mercury intrusion porosimetry (MIP). Please note, that although we use the term pore radius, it is the pore throat, that determines the pressure that is needed to fill the pore behind the bottleneck. The specific surface area (SSA) was determined by means of N_2 gas adsorption based on the Brunauer–Emmett–Teller theory (BET). The software (SOLID) of the MIP unit calculates the specific surface area (SSA) on base of the particle size distribution (Rotare and Prenzlow 1967). The conical model used by the software is accurate for most rock material, although at the same time tuffs are characterized by a considerable amount of bottleneck pores that may be better described by a spherical model. Most importantly, however, the MIP model allows for the identification of relative SSA changes due to the consolidation treatments.

The capillary water uptake (w value) was determined according to DIN EN ISO 15148 on sample cubes of 65 mm edge length in a closed cabinet while weighing over time. On sample discs with a diameter of 40 mm and a thickness of 10 mm the water vapor diffusion resistance (μ value) was measured using the wet-cup method according to DIN EN ISO 12572. The hygroscopic water sorption was measured according to DIN EN ISO 12571 in a climate chamber at 20 °C temperature and relative humidities (RH) between 25 and 95%. Due to time constraints, the relative humidity was increased by 10% every 48 h, while determining the weight difference before every humidity increase.

The ultrasonic P-wave velocity was calculated from the length of cylindrical specimens (50 mm length, 15 mm diameter) and the travel time of ultrasonic P-waves with a frequency of 350 kHz in transmission according to DIN14579. In this study it was also used as a non-destructive tool to obtain the dynamic Young's modulus (E_{dyn}), which is proportional to the rock strength (Siegesmund and Dürrast 2011).

The hydric expansion was measured on cylindrical samples of 50 mm length and 15 mm diameter under conditions of complete immersion in demineralized water, following DIN13009. A displacement transducer with a resolution of 0.1 µm measured the linear expansion as a function of time. Thermal expansion behavior was determined in a climate chamber via pushrod dilatometer and displacement transducer with a resolution of 0.1 µm, following DIN EN 14581. The cylindrical samples of 15 mm diameter and 50 mm length were exposed to two heating and cooling cycles under dry and wet conditions, respectively. In each cycle the dry samples were heated from 20 to 90 °C and subsequently cooled down to 20 °C, with a heating/cooling rate of 1 °C/min. Both minimum (20 °C) and maximum (90 °C) temperatures were hold for 6 h.

Results

Petrography

Geochemically most of the investigated volcanic tuffs are acid rhyolites or trachytes. Only the Weibern tuff (WB) shows an intermediate trachytic to phonolitic composition. After the classification scheme of Schmid (1981) BP, CR, CV, BS and NB can be defined as crystal tuffs. SMA, and HR, can be classified as vitric tuffs and LOS and WB are lithic tuffs (Table 1). Regarding the size of pyroclastic fragments (Fisher 1966), the investigated tuffs are mainly defined as ash tuffs and lapilli tuffs. The crystal rich tuffs are mostly ash tuffs and lapilli tuffs with high ash content. Only the vitric tuffs show higher amounts of lapilli and bombs, which are often present in the form of pumice clasts. Most of the tuffs show considerable amounts of swelling clays and/or an abundance of zeolites. The petrographic and petrophysical properties of the tuffs are compiled in Tables 1, 2 3. In the following, the individual tuffs will be presented in short profiles. Supplementary data (e.g., XRF, XRD, thin section and SEM photomicrographs) can be found in Pötzl (2020).

The Blanca Pachuca (BP) is a fine-grained ash tuff of rhyolitic composition, with a whitish groundmass and plenty of greyish-brownish, rarely reddish and black, phenocrysts that give a slightly speckled appearance (Fig. 3), but cannot be identified macroscopically. In thin section,

Table 1 Petrographic classification of the nine volcanic tuffs

Sample	ID	Origin	Age	Classification LeBas et al. (1986)	Classification Schmidt (1981)	Classification Fisher (1966)
Blanca Pachuca	BP	Mexico	Pliocene	Rhyolite	Crystal	Ash tuff
Cantera Rosa	CR	Mexico	Oligocene	Rhyolite	Crystal	Ash-lapilli tuff
Cantera Verde	CV	Mexico	Miocene	Rhyolite	Crystal	Ash tuff
Blue Sevan	BS	Armenia	Cretaceous	Rhyolite	Crystal	Ash tuff
Noyemberyan	NB	Armenia	Cretaceous	Rhyolite	Crystal	Ash tuff
San Miguel el Alto	SMA	Mexico	Paleogene	Rhyolite	Vitric	Lapilli tuff
Hoktemberyan Red	HR	Armenia	Pleistocene	Trachyte	Vitric	Lapilli tuff
Loseros	LOS	Mexico	Oligocene	Rhyolite	Lithic	Ash tuff
Weibern	WB	Germany	Pleistocene	Phonolite	Lithic	Lapilli tuff

quartz, potassium feldspar, plagioclase, biotite and clay minerals can be observed in a cryptocrystalline matrix. XRD identified swelling clays (smectite) and a range of zeolites (mordenite, heulandite, clinoptilolite). SEM photomicrographs show mordenite needles reaching into the pore space. Overall, the glassy matrix is mainly altered to zeolite and clay. BP has a notably high cation exchange capacity (CEC) of 12 meq/100 g and specific surface area (SSA) of 17m^2/g (Table 2). The former glass rich BP is, due to alteration processes, now characterized as highly rich in clay and zeolite crystals. After the classification system of Schmid (1981) and Fisher (1966), BP categorizes as crystal-rich ash tuff (Table 1).

Cantera Rosa (CR) is a massive, crystal rich, rhyolitic tuff of characteristic pinkish color. It macroscopically and microscopically shows a porphyritic texture, with large amounts of quartz and feldspar phenocrysts as well as pumice clasts of up to 20 mm in size, embedded in a fine cryptocrystalline groundmass (Fig. 3). In thin section, quartz and sanidine crystals are especially abundant. In SEM photomicrographs the groundmass shows to be altered and devitrified and now consists of a mix of clay, quartz and feldspar crystals. XRD identified the clay minerals as swellable smectite, as well as muscovite/illite and kaolinite. The CEC is accordingly increased (6 meq/100 g). CR is classified as crystal tuff according to Schmid (1981) and as lapilli rich ash tuff according to Fisher (1966).

The Loseros tuff (LOS) is characterized by a greenish laminated appearance (sometimes with a slightly purple or reddish tint), which is mainly caused by sand-sized crystals and rock fragments embedded in a fine, ash-rich matrix (Fig. 3). LOS is of rhyolitic composition and classifies as lithic ash tuff (Fisher 1966; Schmid 1981). In thin section, the main components are identified as lithic fragments, as well as quartz, feldspar and plagioclase phenocrysts, whereby the lithic components dominate. LOS contains around 10% of opaques and shows chloritization phenomena. The individual grains are cemented with a calcareous and argillaceous matrix. XRD identified smectitic mixed-layer minerals and kaolinite. SEM analyses located the clay minerals preferably at grain contacts. LOS shows a moderately high CEC of 5 meq/100 g (Table 2).

The rhyolitic San Miguel el Alto tuff (SMA) consists of a fine and homogenous vitric groundmass of characteristic pinkish color, in which plenty of elongated pumice clasts are embedded (Fig. 3). The pumice clasts are typically in the millimeter to centimeter range and indicate direction. In thin section, SMA shows an abundance of small quartz and feldspar crystals, embedded in a glass rich matrix. XRD identified rare kaolinite-smectite mixed-layer minerals, which are abundant in SEM photomicrographs. Glass shards and biotite are rarely seen. With 4 meq/100 g, the CEC is moderately high. According to Schmid (1981) and Fisher (1966), SMA can be classified as vitric lapilli tuff.

Cantera Verde (CV) is a relatively homogenous, light-pistachio green, crystal-rich ash tuff (according to Fisher (1966) and Schmid (1981)) of rhyolitic composition. Macroscopically noticeable are white clay lenses (Fig. 3), which partly disintegrate when in contact with water. CV has a hypocrystalline to cryptocrystalline matrix with vitrophyric texture. The vitreous matrix, however, is strongly altered to zeolite (clinoptilolite and mordenite) and clay minerals (smectite, illite, chlorite and potentially kaolinite). Phenocrysts are often strongly weathered. SiO_2 is present in the form of cristobalite. De Pablo-Galán (1986) describes the formation of zeolites in CV by alkaline diagenesis of rhyolitic glass. SEM photomicrographs reveal very fine-grained zeolites in CV, causing its high specific surface area (26 m^2/g). They are mainly euhedral mordenite needles and clinoptilolite laths.

The Blue Sevan (BS) has a characteristic intense green color and is of rhyolitic composition. It is very fine-grained and bottle-green elongated fragments, in the micrometer to millimeter scale, indicate a lamination (Fig. 3). In thin section, this tuff shows about 80% cryptocrystalline matrix, with few mono- and polycrystalline quartz crystals as well

Table 2 Mineralogical composition (XRD), cation exchange capacity (CEC) [meq/100 g] and specific surface area (SSA) by N_2 adsorption

sample	CEC (meq/100 g)	SSA (m^2/g)	Clay minerals						Zeolites				Other								
			Smectite	Smectitic mixed layer	Corrensite	Muscovite/illite	Chlorite	Kaolinite	Mordenite	Heulandite	Clinoptilolite	Analcime	Glass/amorphous	Quartz	Tridymite	Cristobalite	K-feldspar	Plagioclase	Hematite	Augite	Hornblende	Calcite
BP	12	17	xx						x	xx	x			xx		x	x	x				
CR	6	5	xx			x		x						xx			x	x				
LOS	5	12		xxx				x						x			x	x				x
SMA	4	7		xx										xx	x		x	xx				
CV	6	26	x			x	x	?	x	xx						xx	xx					
BS	9	8		xx		x		x				x		x			x					
HR	1	1				?							xx	x			xx		x			
NB	9	3		x		x			x					x			x			x		x
WB	5	14				x						xx		x			xx	x				x

The x's display the semiquantitative occurrence of the minerals. xxx: dominating mineral phase, xx: major component, x: minor component, ?: trace phase possibly present

as feldspar phenocrysts embedded. The bottle-green fragments often show chloritization processes. In SEM photomicrographs, huge amounts of frayed edge clay minerals are oriented parallel to the bedding. They are located both at grain contacts and mixed into the fine-grained matrix consisting of quartz and feldspar. XRD of separated clay fractions identified them as intracrystalline swellable smectites (Table 2). Illite/muscovite, kaolinite and analcime, a mineral of the zeolite group, could also be identified. Huge apatites and feldspar relics as well as muscovites can occasionally be observed. The CEC is very high (9 meq/100 g). BS is classified as crystal-rich ash tuff according to Fisher (1966) and Schmid (1981).

The Hoktemberyan Red (HR) has a striking brick-red color and chemically classifies as trachyte. In its glass rich ground mass, huge amounts of elongated white feldspar phenocrysts and glass particles are embedded and give a slightly speckled appearance (Fig. 3). Black and red elongated pumice at the millimeter to centimeter scale, are embedded in the groundmass and indicate an orientation. In thin section, HR shows feldspar and amphibole phenocrysts embedded in a high amount of glassy matrix (~75%), with high amounts of iron oxides. Volcanic lithoclasts and opaque minerals each make about 5% of the sample. In SEM photomicrographs, the difference in porosity between matrix and clasts is striking. Huge parts of these consist of amorphous glass and especially in the matrix area, tiny pores are present. Rarely clay minerals with characteristic frayed edges in the pores of the glassy matrix are observed. HR shows a low CEC (1.2 meq/100 g) and SSA (1 m^2/g). HR is classified as vitric lapilli tuff (Fisher 1966; Schmid 1981).

The Noyemberyan tuff (NB) is a massive, white to slightly greenish tuff of rhyolitic composition, which shows a weak lamination in form of white and grey elongated lithic fragments (Fig. 3). Many of the grey lithic fragments are framed by slightly orange to reddish margins. Macroscopic, NB appears to be a fine-grained tuff. Only in exceptional cases the lithic fragments reach sizes up to one centimeter. Thin section images confirm the large amounts of fine matrix groundmass (70%). The remaining 30% of the rock consist of partly large angular and zoned plagioclase crystals as well as small, rounded quartz fragments. SEM photomicrographs identify huge amounts of fibrous mordenite clusters and frayed edge clay minerals. Calcites and muscovites can reach dimensions up to 300 µm. Rarely apatite can be observed. Huge amounts of mordenite, a mineral of the zeolite group, and intracrystalline swellable smectitic layers in an illite–smectite mixed layer mineral were identified by XRD on separated clay fractions and confirm a moderate CEC of 3.1 meq/100 g. The classification system after Schmid (1981) and Fisher (1966) categorize NB as crystal-rich ash tuff.

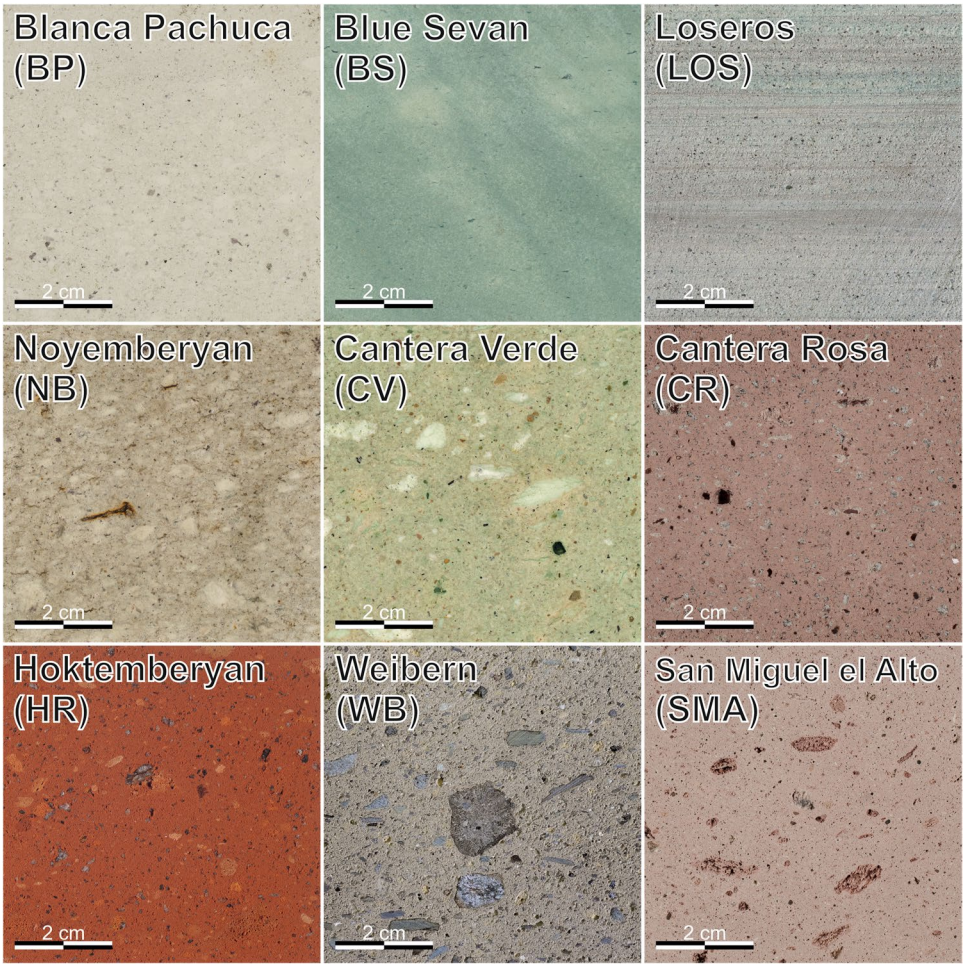

Fig. 3 Macroscopic photographs of the nine volcanic tuffs from Armenia, Germany and Mexico

The Weibern tuff (WB) is of trachytic to phonolitic composition. In the literature, the reported composition of WB is usually phonolitic (Poschlod 1990; Egloffstein 1998; Stück et al. 2008). It has a characteristic fine-grained, yellowish to brownish groundmass, in which plenty of partly elongated volcanic and sedimentary clasts are embedded (Fig. 3). Beside basalt, chert and sandstone clasts on the centimeter scale, yellowish pumice clasts of few millimeter size are abundant. Quartz, feldspar, leucite, calcite, hornblende and biotite could be identified in thin section. Some opaque minerals could not be identified. In thin section, also the high amount of lithics is striking (~40%). Other authors report far less lithic components and higher amounts of vitric groundmass (Egloffstein 1998; Stück et al. 2008; Wedekind et al. 2013). These authors did also report significantly smaller sizes for the embedded rock fragments. SEM analyses were not conducted on WB. However, XRD analyses identified an abundance of zeolite material (analcime) and potential smectitic mixed-layer minerals, which points to the fact that the vitric groundmass of the tuff is already altered, like reported by van Hees et al. (2003). The CEC is moderately high (5 meq/100 g), the SSA is very high (14 m^2/g). WB can be classified as lithic lapilli tuff according to Schmid (1981) and Fisher, (1966). The boundary, however, is fluid, since we did not determine the cryptocrystalline groundmass any further by SEM, it as well may not be altered to zeolite yet and therefore classify as vitric tuff.

Quantitative absorption of TEOS and TMOS

The quantitative absorption of the consolidants was indirectly determined by dry weight measurements of the cylindric samples (50 mm length, 15 mm diameter) before and after the treatment. The weight measurements were conducted after 6 weeks of storage at 23 °C/60% RH (85% RH for TMOS), for full curing of the consolidants. After 6 weeks the samples were dried in an oven at 40 °C until constant mass was achieved and subsequently equilibrated at room temperature for one hour. Figure 4 displays the respective increase in weight percentage of each sample.

The consolidation with TMOS in any combination lead to a significant higher weight increase than TEOS, indicating a general stronger absorption and gel deposition

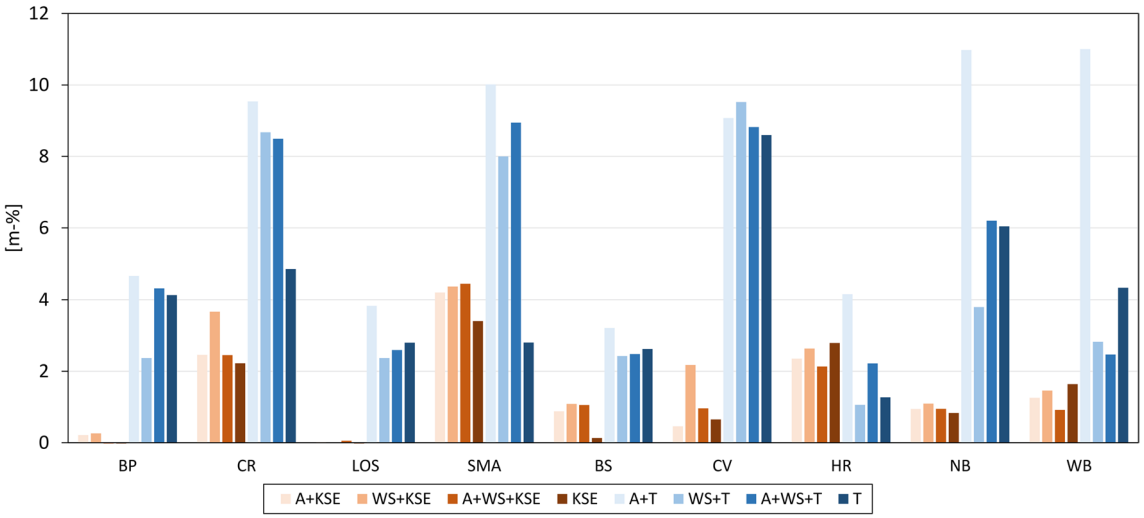

Fig. 4 Quantitative absorption of the consolidants by dry weight change of the sample before and after the treatment

rate of TMOS. Only in HR the application of TEOS with Antihygro pretreatment (A + KSE) lead to a higher absorption. The difference between both consolidants is especially striking for the comparatively low porous tuffs with a high fraction of micropores, like BP, LOS, CV and NB. The combination of TMOS with Antihygro (A + T) turned out to be most effective. The application of TEOS shows the strongest increase in combination with tartaric acid (WS + KSE/A + WS + KSE) for most tuffs.

The extremely low absorption of TEOS by BP and LOS may represent an analytical artifact from their specific pore space characteristics, which regulate the water absorption of the stone. Both tuffs contain considerable amounts of swelling clays and/or zeolites, causing a distinct occurrence of nanopores (Tables 2, 3) that lead to a high hygroscopic water sorption potential already at low humidities. A possible interpretation would be that BP and LOS already absorb considerable amounts of moisture from the ambient humidity during the one hour temperature equilibration outside the oven. In doing so, their subsequently determined dry weight before the treatment would be increased and an absorption of the consolidant in terms of weight difference before and after accordingly reduced.

Aesthetic changes

If possible, the visual appearance of the tuffs should not be changed through a consolidation treatment. A darkening of the stone is, however, a common side effect of many consolidation measures and may diminish over time (Nishiura 1987; Wheeler and Newman 1994). If that is not the case, the consolidation product may be considered inappropriate (Snethlage and Sterflinger 2011).

In this study both consolidants cause different aesthetic changes. The application of TEOS, especially in combination with Antihygro, leads to partial darkening of the highly porous tuffs. The effect is most striking in WB, SMA and CR (Fig. 5). TMOS causes a partial darkening of all tuffs. Compared to TEOS the effect is less intense on the highly porous tuffs. However, the combination of TMOS with anti-swelling agent and tartaric acid (A + T/A + WS + T) leads to a glossy appearance on the surface of BP, CV and CR (Fig. 6). The glossy appearance may indicate that the moisture content during the application was too high, so that the silica gel already precipitates at the surface of the specimen (Snethlage and Sterflinger 2011). The humidity conditions during the application of TMOS (75% RH preconditioning; 85% RH storage) in combination with the Antihygro on the low porous tuffs BP, CV and CR consequently have to be evaluated as inappropriate.

Another unfavorable side effect is the occurrence of salt efflorescence on the highly porous SMA, HR and WB after treatment with Antihygro (Fig. 6). These salts do not only have an unpleasant aesthetic effect, but also influence the petrophysical properties of the tuffs, as will be seen in the following sections. Note, that the samples were not desalinated before the consolidation treatment. Since none of these three tuffs did show significant hydric expansion in an untreated condition, the treatment with Antihygro was not necessary in the first place. As the Antihygro could not interact with any clay minerals, it potentially led to an excessive supply of salt that migrated to the surface. This underlines the importance of constant benefit-risk assessment prior to an intervention.

Table 3 Summary of the technical parameter of the untreated volcanic tuffs

Sample ID	BP	CR	LOS	SMA	BS	CV	HR	NB	WB
Porosity [vol%]	14.9	31.1	16.8	40.8	14.9	29.5	33.1	25.7	36.9
Bulk density [g/cm^3]	1.85	1.78	2.07	1.52	2.06	1.54	1.62	1.73	1.51
Matrix density [g/cm^3]	2.17	2.58	2.49	2.57	2.42	2.18	2.43	2.34	2.40
Water absorption vac. [wt%]	8	18	8	27	7	19	20	15	24
Water absorption atm. [wt%]	7	14	7	17	6	16	15	13	20
Saturation coefficient S	0.86	0.77	0.81	0.65	0.83	0.85	0.75	0.87	0.84
Micropores [%]	79	18	85	10	90	88	4	37	14
Capillary pores [%]	21	82	15	90	10	12	96	63	86
Mean pore radius [µm]	0.05	0.52	0.04	1.50	0.03	0.04	3.93	0.14	0.51
SSA via BET [m^2/g]	17	5	12	7	8	26	1	3	-
SSA via MIP [m^2/g]	9.7	5.1	9.6	4.7	4.0	20.8	1.8	6.5	9.7
CEC [meq/100 g]	12	6	5	4	9	6	1	9	-
w-value [kg/m^2 $\sqrt{h}$]									
X	0.8	9.4	0.8	7.3	0.8	2.8	45.1	3.9	14.9
Z	0.8	7.1	0.7	4.7	0.5	2.6	31.0	3.8	14.2
μ-value									
X	11.9	7.5	27.9	7.4	14.4	9.2	8.1	14.4	9.1
Z	11.1	8.4	13.4	8.1	14.2	10.1	9.7	14.5	9.1
Sorption 95% RH [wt%]	4.5	2.6	2.9	1.2	2.9	7.9	0.1	3.5	3.2
ø hydric exp. [mm/m]									
X	0.71	0.10	0.58	0.07	0.35	1.39	−0.07	0.67	0.56
Z	0.96	0.24	1.22	0.23	1.57	1.68	−0.13	0.76	0.65
MAX	1.14	0.29	1.78	0.34	2.52	2.01	−0.16	0.97	0.66
ø α [10^{-6} K^{-1}] dry									
X	13.4	8.5	9.8	8.8	8.3	10.9	6.3	8.4	5.9
Z	13.4	8.6	11.7	9.4	10.2	10.6	7.0	7.5	6.8
Resid. strain ε *X* [mm/m]	0.16	−0.03	−0.03	0	0.05	−0.45	−0.01	0.05	0.05
Resid. strain ε *Z* [mm/m]	0.17	−0.02	0.05	2E−05	0.08	−0.36	−0.005	0.07	0.07
ø α [10^{-6} K^{-1}] wet									
X	23.6	9.5	12.9	10.7	14.1	47.2	8.5	27.0	13.9
Z	24.2	9.7	32.1	12.0	27.1	50.7	7.2	26.7	18.7
Resid. strain ε *X* [mm/m]	−0.08	0.04	−0.01	0.07	−0.16	−0.05	−0.08	0.13	0.06
Resid. strain ε *Z* [mm/m]	−0.10	0.04	−0.74	−0.03	−0.51	−0.21	−0.005	0.07	0.07
P-wave velocity [km/s]									
X	3.3	2.8	3.7	2.7	3.9	2.7	2.9	3.1	2.5
Z	3.2	2.6	2.8	2.3	3.1	2.6	2.3	3.2	2.5
Young's Modulus [GPa]									
X	20	14	28	11	31	11	14	17	9
Z	19	12	16	8	20	10	9	18	9

X parallel to the bedding, *Z* perpendicular to the bedding, *SSA* specific surface area, *CEC* cation exchange capacity, α coefficient of linear thermal expansion

Modification of petrophysical properties

The consolidation treatments modified properties like pore space properties and water transport mechanisms and therefore the strength and durability to varying degrees (Table 3). A comparison of the petrophysical properties and expansional behavior before and after the treatment for each individual tuff can be found in Tab.E1–9 in the electronic supplementary material (ESM).

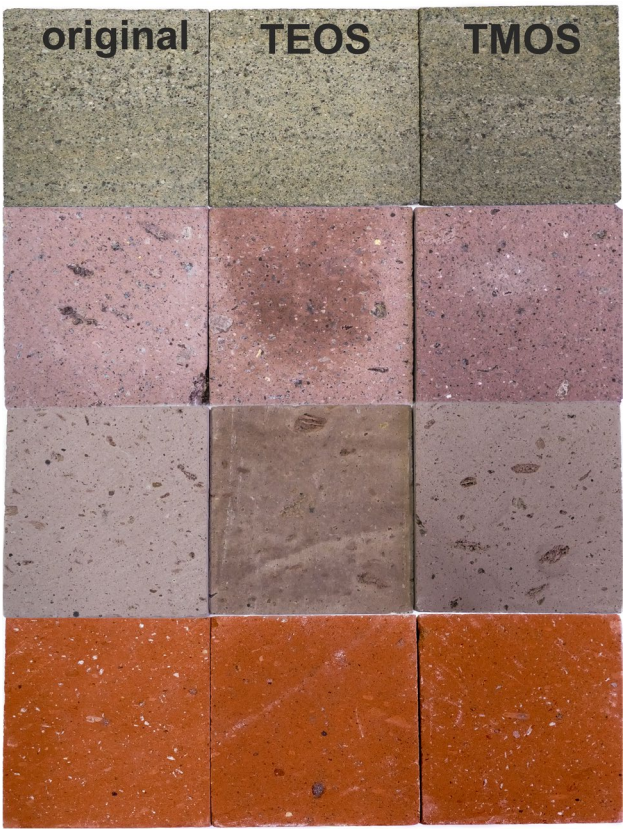

Fig. 5 Comparison of visual appearance of untreated (left row) sample cubes (65 mm edge length) with cubes treated with TEOS (middle row) and TMOS (right row). Examples of LOS, CR, SMA and HR (from top to bottom)

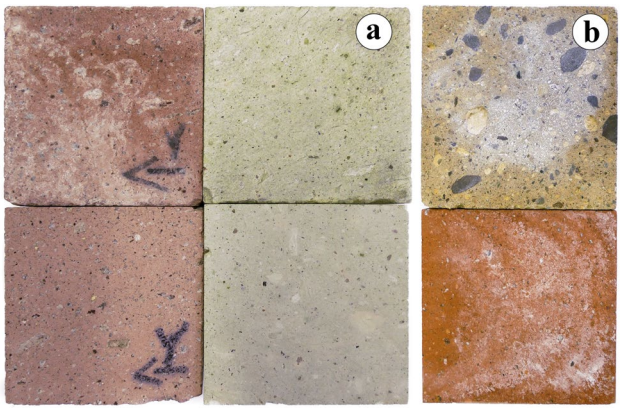

Fig. 6 **a** Glossy appearance of CR and CV (top) compared to the untreated sample (bottom). **b** Salt efflorescence as a result of the treatment with Antihygro in WB (top) and HR (bottom). Sample cubes of 65 mm edge length

Modification of pore space properties

Porosity

The deposition of the consolidant in the pore space inevitably leads to a reduction of the effective porosity. The reduction takes place to varying degrees in the different types of tuff and appears to be especially extreme for the less porous tuffs. BP, BS and LOS are characterized by moderate porosities of 15–17 vol%. The other tuffs show significantly higher porosities between 26 and 41 vol%. With one exception (TEOS only on BS) all treatments successfully decreased the porosity of the stones (Fig. 7). For TEOS, the treatment in combination with the tartaric acid (WS + KSE/A + WS + KSE) was most efficient, while the treatment with TMOS showed the strongest effects in combination with the Antihygro or when applied solely (TMOS/A + T). Substantial reduction of the porosity of NB was only achieved by consolidation with TMOS (especially A + T). In general, TEOS showed to be slightly more effective on highly porous tuffs, while TMOS showed more pronounced changes for tuffs with lower porosity. Some extreme porosity reductions between 60 and 80% were achieved by TMOS treatment on BP, BS and LOS. However, these strong reductions may be owed to the sealing of the pore channels by the silica gel and the creation of an inaccessible porosity.

Pore radius

Tuffs with a high share of micropores proved to be especially susceptible to weathering (Pötzl et al. 2018b) and because micropores (< 0.1 µm) have a strong influence on the drying behavior of rocks, a reduction of micropores is highly desirable. The fraction of micropores in BP, LOS, BS and CV (79–90%) is significantly higher than in the other tuffs (< 37%) (Tab.E1–9 in the ESM). The deposition of the consolidant in the pore space does visibly change the fraction of micropores and thus the pore size distribution of the tuffs to varying degrees, and depending on the applied consolidant, in opposite directions. While treatment with TEOS generally decreases the share of micropores and thus increases the mean pore radii (with the exception of HR), the application of TMOS in any form usually increases the fraction of micropores and decreases the mean pore radii. For an overview the general trends are displayed in Fig. 7, but the effect of the different treatments on the pore size distributions become more apparent, when looking at the pore size histograms of the individual tuffs (Fig.E1–3 in the ESM).

The most striking observation in nearly all consolidation treatments is the shift of the most occurring pore class

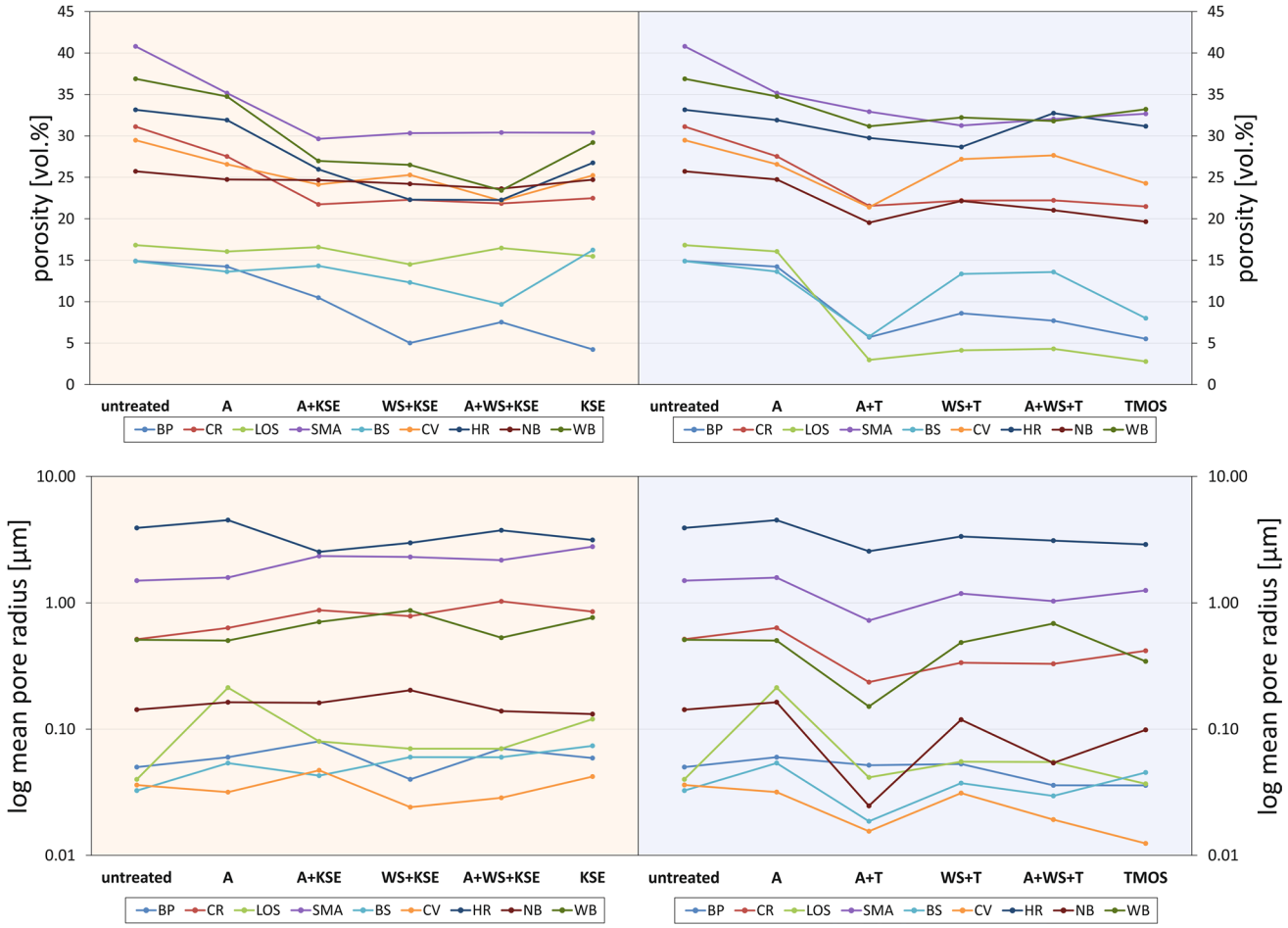

Fig. 7 Modification of the effective porosity and mean pore radii due to the consolidation treatments. Left) TEOS, right) TMOS. Due to the wide range of values, the mean pore radii are displayed on a logarithmic scale

in opposite directions, depending on the applied consolidant. These shifts are especially striking in low to moderately porous tuffs, like BP, BS, LOS, CV and NB, and most intense when consolidated with TMOS. With the exception of CV pretreated with tartaric acid, the consolidation with TEOS results in a peak shift of one or two pore classes towards larger pores (Fig. 8; please find the figures for the other tuffs in the electronic supplements). The intensity of the shift, however, does not seem to strongly differ by a combinational treatment with tartaric acid or anti-swelling agent. Treatments with TEOS do not result in a significant redistribution of pore classes.

In contrast, tuffs consolidated with TMOS in any combinational treatment experience a strong shift towards smaller pores and in doing so, a partly strong redistribution of the occupied pore classes. The shift is not only happening on the scale of one or two classes, like observed in samples treated with TEOS, but rather up to six or seven pore classes (e.g., CV). A common outcome is a highly increased fraction of micropores on the single-digit nanometer scale, which in turn correlates with an increased specific surface area (SSA) that is subsequently available for additional adsorption processes and chemical interaction (see Tab.E1–9 in the ESM). Figure 9 shows clear trends of decreasing SSA due to TEOS treatment and partly strong increase of SSA due to the consolidation with TMOS. Especially the combination of TMOS with Antihygro (A + T/A + WS + T) leads to some extreme doubling, tripling or even quadrupling of the SSA.

In some cases, the redistribution of the pore size changes the whole pore character of the tuff. According to the pore radii distribution type model of Ruedrich and Siegesmund (2006), SMA and HR are characterized as unimodal equal pore radii type (Type A), BP and NB are characterized as unimodal unequal pore radii type (Type B) and the rest is characterized as bimodal pore radii type (Type C). In Fig. 8 (and Fig.E1–3 in the ESM) it can be observed that the strong shift of occupied pore classes in BP, NB, SMA and HR changes the distribution type from unimodal to bimodal (and partly trimodal). In bimodal pore radii types the distribution usually shows a flattening effect, due to a relative decrease

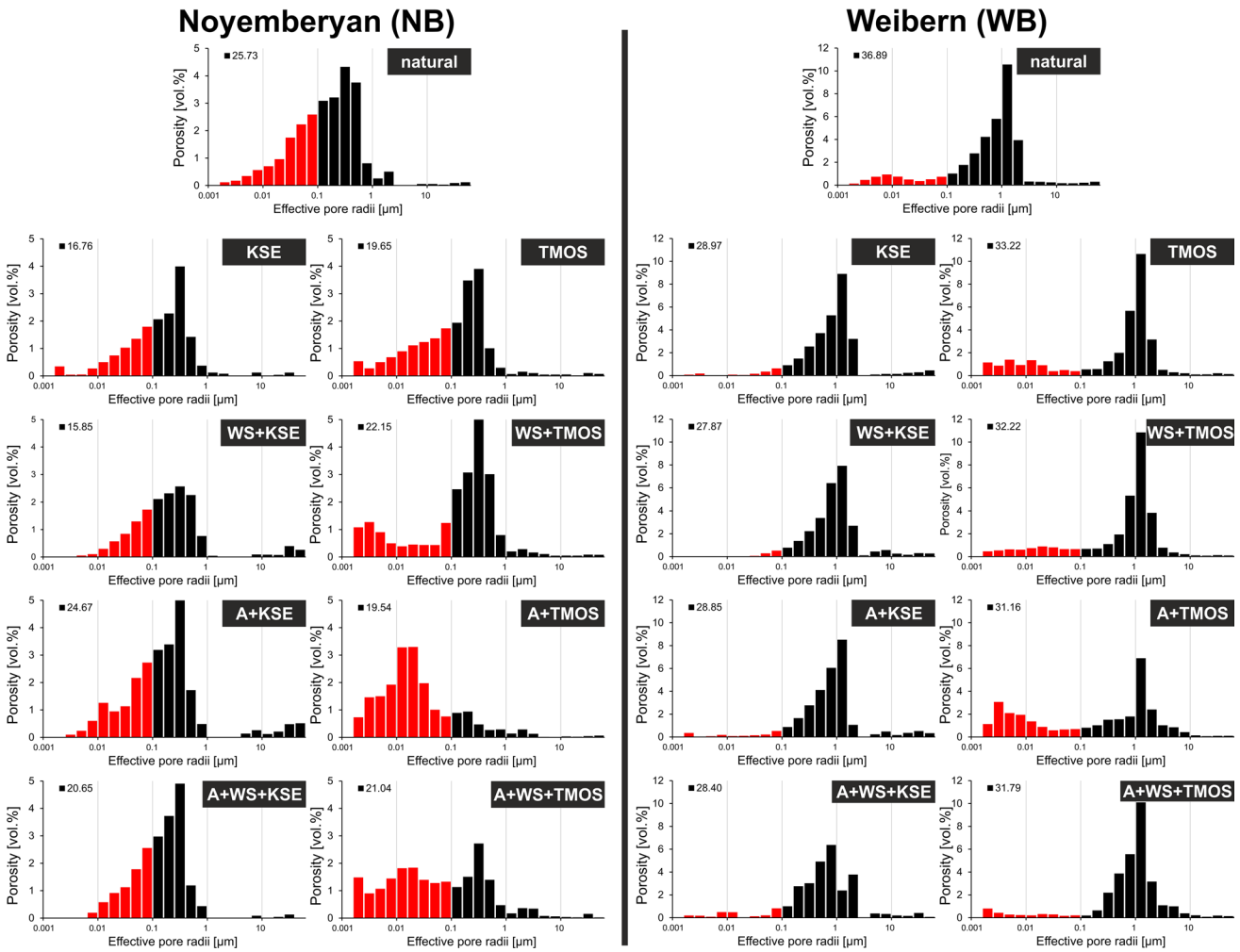

Fig. 8 Modification of the pore radii characteristics of NB and WB due to the consolidation treatments. Left row) TEOS, right row) TMOS; red = micropores, black = capillary pores

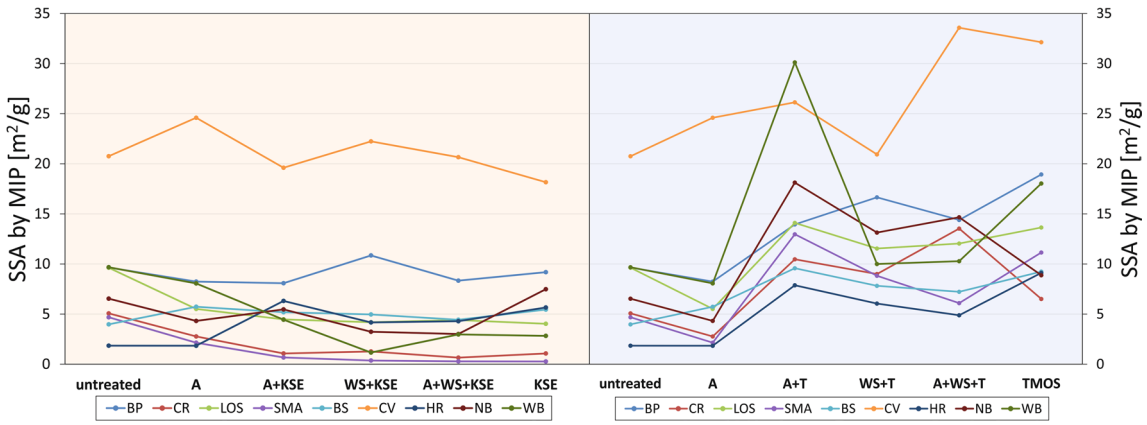

Fig. 9 Modification of the specific surface area (SSA) due to the consolidation treatments, derived from the mercury intrusion porosimetry (MIP). Left) TEOS, right) TMOS

of the higher peak and a simultaneous increase of the lower peak. A good example for this effect is WB (Fig. 8). The flattening effect may also be increased in some tuffs by a divergent shift of pore classes. While the main share of pores moves in direction of smaller pore radii, a small fraction shifts towards larger capillary pores (e.g., in CV; see Fig. E2 in the ESM). This way the tuffs maintain the ability of capillary water transport inside the stone, while increasing their ability for water retention in pores < 0.1 µm. The shift towards capillary pores is most likely the result of the narrowing of larger pores that were previously outside the analysis spectrum. Bimodal pore size distributions in tuffs have been evaluated critically in the literature (Wedekind et al. 2013; López-Doncel et al. 2016; Pötzl et al. 2018a, b), amongst others because of their increased risk of susceptibility towards salt weathering and hydric expansion.

Modification of the water transport and retention properties

A strongly water absorbing stone should ideally also show a high water vapor permeability, so that after a fast/intense water absorption (e.g., due to a rain event) the stone has the ability to dry equally fast (Snethlage and Pfanner 2020). However, due to their partly high fractions of micropores, tuffs tend to retain the water in their pore space for a considerable amount of time.

Capillary water absorption and water vapor diffusion resistance

The low porous tuffs BP, BS and LOS show comparatively low capillary water absorption (w value < 1 kg/m$^2\sqrt{\text{h}}$) and high water vapor diffusion resistance (µ value). Water transport in both directions is accordingly low for these tuffs. NB and CV show moderate w values of up to 4 kg/m$^2\sqrt{\text{h}}$ and moderate to high water vapor diffusion resistance. Considering their pronounced capillary water absorption, these tuffs may retain the water for too long and inhibit an effective drying. CR, SMA and WB show high capillary water absorption, with w values between 5 and 15 kg/m$^2\sqrt{\text{h}}$. They also show appropriately reduced μ values that may balance an intense water uptake. It is, however, striking that SMA with the highest porosity (41 vol%) and a fraction of 90% capillary pores, does show lower capillary water uptake than WB and CR. Especially perpendicular to the bedding (in Z direction) the water uptake is significantly reduced, which points to a rather poorly connected pore network. With up to 43 kg/m$^2\sqrt{\text{h}}$, HR shows by far the highest capability of capillary water uptake (Tab. 3). Its μ value is comparably low and should allow for a considerably fast drying.

Depending on the type of tuff and the applied consolidation measure, the water transport and retention properties of the tuffs change in parts dramatically and confirm the findings regarding the pore space properties made in the previous section. Low porous tuffs consolidated with TMOS tend to show a stronger reduction of their total water absorption under atmospheric conditions and capillary water absorption, while for highly porous tuffs these values could be reduced more effectively with TEOS (Fig. 10). When applying TEOS, the combination with the tartaric acid proved to be most effective, while the consolidation with TMOS proved to be most effective in combination with the anti-swelling agent. However, with the exception of BS and CV, the water transport properties of the tuffs were more strongly influenced by the treatment with TEOS. This may be due to the hydrophobic effect of some ethyl groups that did not react during the gelation. A temporary hydrophobic effect of TEOS is somewhat expected and may diminish over time (Doehne and Price 2010). A residual hydrophobicity of TEOS can be removed in the short term by 2–4 treatments with 1:1 v/v solutions of ethanol:water, which, however, was not done in this study. Samples that were treated with tartaric acid prior to the TMOS/TEOS application, exhibit better water transport properties, which is likely the result of the residues of the acid that cause preferential hydrolysis of the ethoxy groups and therefore reduces or eliminates the hydrophobicity. If a hydrophobic effect does not apply, the strong reduction of the capillary water absorption as well as extreme increase of water vapor diffusion resistance may point to a significant narrowing of pathways and reduced accessibility of liquids to the pore network. While the decreasing capillary water absorption fits the catalog of requirements after Snethlage and Pfanner (2020), the strongly increasing water vapor diffusion resistance in most consolidated tuffs often surpasses the maximum recommended increase of the μ value ($\leq$ 20%) (Fig. 11). Since the creation of a diffusion barrier is to be avoided by all means, most treatments have to be evaluated critically in this regard. The fact that CV and CR still show the ability of water transport, suggests that the previously mentioned glossy coating after the TMOS treatment in combination with Antihygro does at least not seal the pore entries and pathways. In fact, Antihygro exhibits a basic pH of 8.5 and higher pHs promote rapid condensation and gelation, which might be responsible for the gloss in the TMOS samples, as TMOS can react much more quickly than TEOS. General remark: please note, that Snethlage and Pfanner (2020) highlight that the critical values of their catalog of requirements should not be considered as unconditional, rigid rules, but rather as recommendations based on scientific findings and experience on stone consolidation of the last decades.

A pronounced anisotropic behavior of the tuffs, with usually higher capillary water absorption and lower water vapor diffusion resistance parallel to the bedding plane (X direction) indicates a better connection of the pore network in

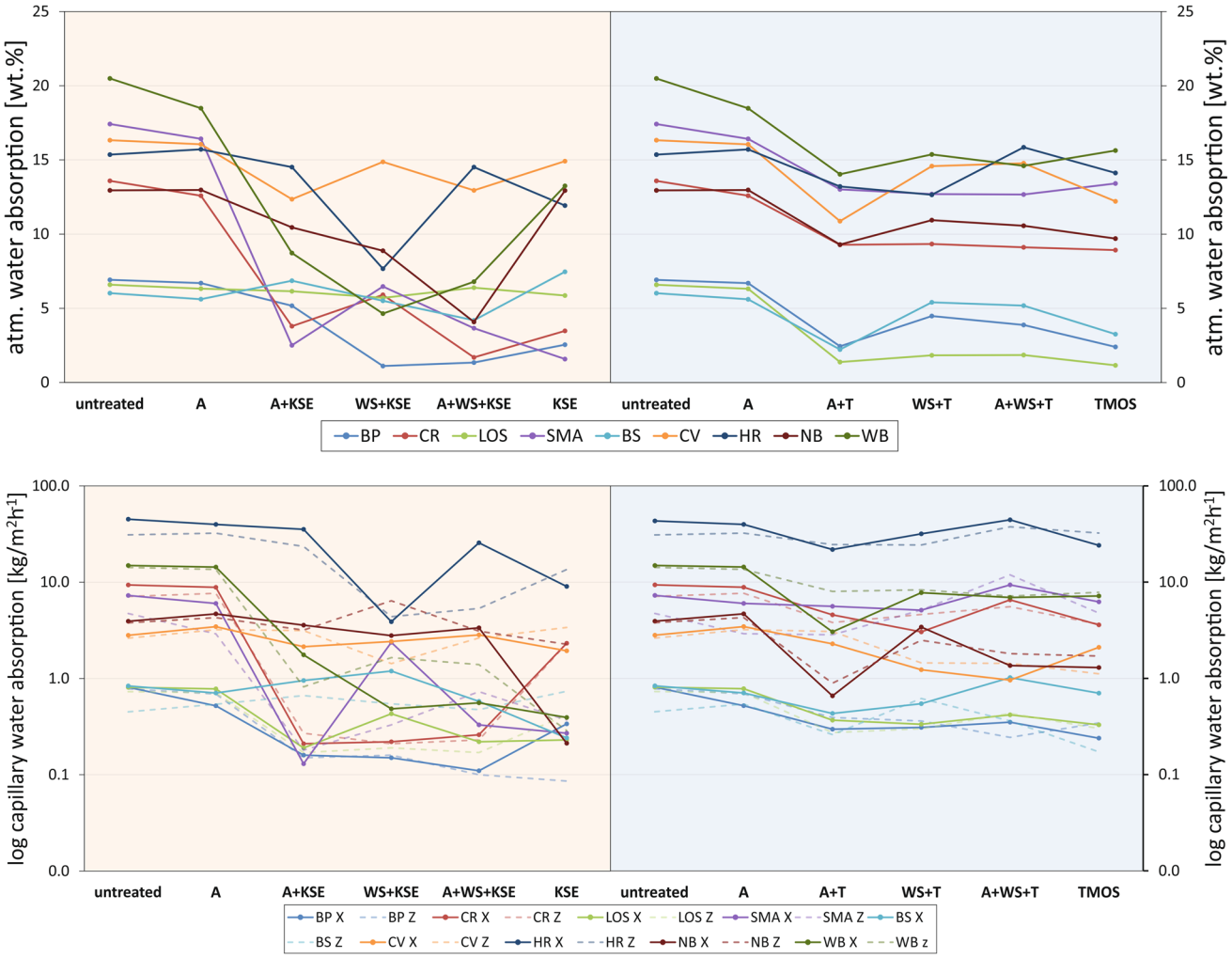

Fig. 10 Modification of the total water absorption under atmospheric conditions and the capillary water absorption due to the consolidation treatments. Left) TEOS, right) TMOS

this direction. The pathways perpendicular to the bedding plane (Z direction) seem to be more poorly developed, by showing half the capillary water uptake and double the water vapor diffusion resistance in some samples (see Tab.E1 –9 in the ESM).

Hygroscopic water sorption

The nine investigated tuffs show diverse potential for moisture absorption from the air (Figs. 11–13). Considering their high total water absorption potential under full imbibition, untreated HR and SMA show very low hygroscopic water sorption of 0.1 and 1.2 wt%, respectively. High hygroscopic water absorption of 7.9 wt% is shown by CV, while the rest of the tuffs show moderate values between 2.6 and 4.5 wt%. The highest values are thereby shown by tuffs that are rich in zeolites and swelling clay minerals (compare Table 2). The adsorption isotherms of the untreated tuffs in Figs. 12 and 13 generally show a significant increase of hygroscopic water sorption between 75 and 95% relative humidity (RH). BP and LOS show already a considerably increased adsorption at low relative humidities.

Except for the low porous tuffs BP, LOS and BS, the consolidation measures changed the absorption behavior drastically and these drastic changes correlate very well with the modification of the pore size distribution (Fig. 8; Fig.E1–3 in the ESM). A representative example is CR, whose fraction of micropores was decreased by TEOS treatments, so that TEOS treated CR shows decreased hygroscopic water sorption potential (Fig. 12). Another reason for a decreasing hygroscopic water sorption may be a narrowing or sealing of the pathways, which potentially inhibits further absorption. On the other hand, the increasing fraction of micropores due to TMOS treatments subsequently leads to an increasing hygroscopic water sorption of CR. It is striking that the strongest increase of hygroscopic water sorption is often

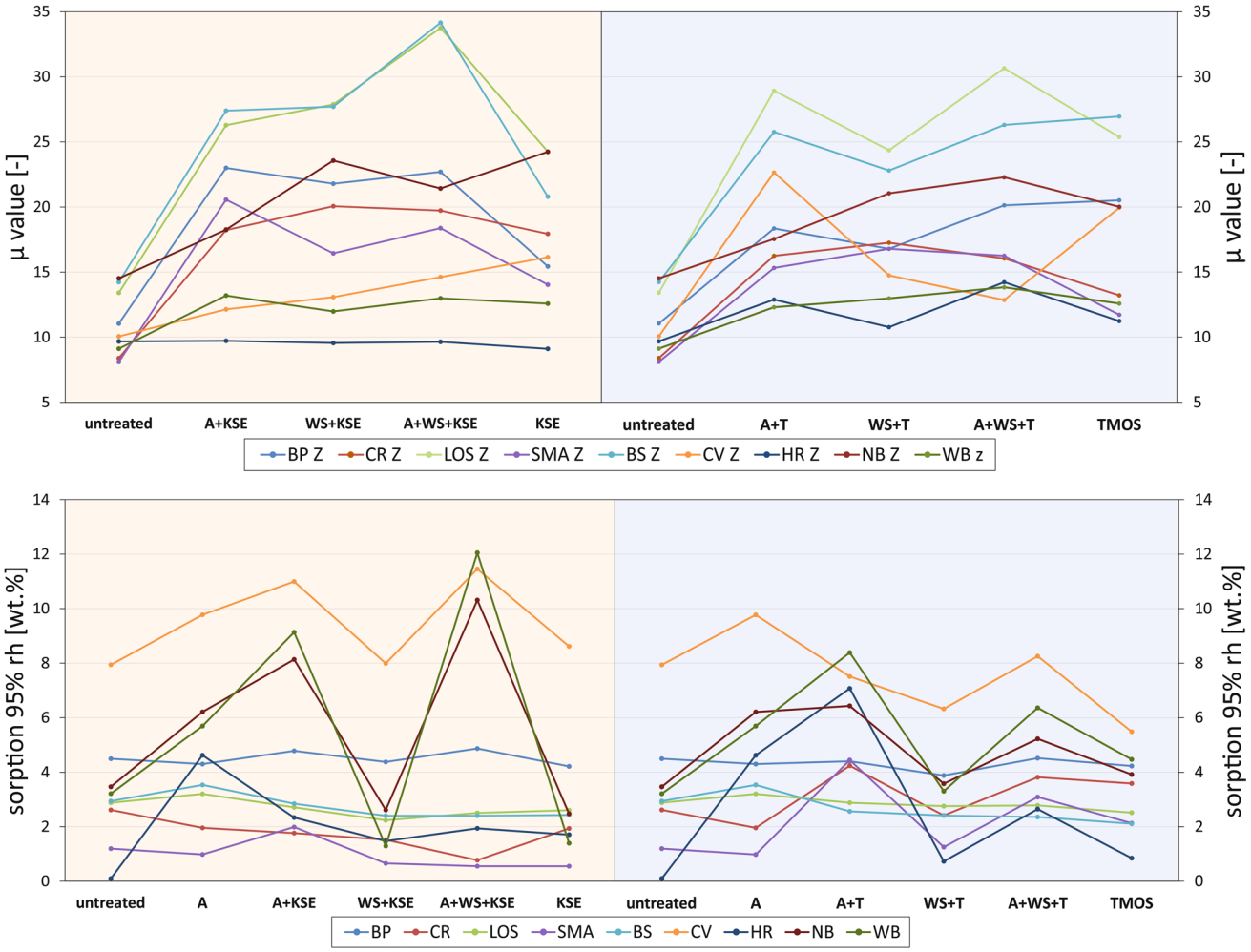

Fig. 11 Modification of the water vapor diffusion resistance coefficient μ and the maximum hygroscopic water sorption value at 95% relative humidity due to the consolidation treatments. Left) TEOS, right) TMOS

connected to a pretreatment with the anti-swelling agent. The ion exchange with the anti-swelling agent may have led to the formation of hygroscopic salts. Particularly HR, SMA and WB, which showed minor salt efflorescence after the application of the anti-swelling agent, demonstrate this very clearly. Hygroscopic salts are known to efficiently adsorb moisture from the air and may therefore be responsible for the increased hygroscopic water sorption behavior of the addressed samples. The hygroscopic nature of salts is further discussed in Steiger et al. (2011).

Modification of the expansional behavior

Hydric expansion

Apart from HR and WB, swelling clays were identified in all investigated tuff stones, so that moisture expansion most likely plays a role in their deterioration. A general observation is an ubiquitous anisotropic expansional behavior of all tuffs with distinct higher expansion in the Z direction (perpendicular to the bedding) (Table 3). Extreme examples are BS and LOS, showing anisotropies of up to 78%. In the following, the expansional behavior in Z direction will be representatively discussed (Fig. 14).

CR and SMA show considerably low hydric expansion of around 0.2 mm/m when compared to WB (0.7 mm/m) and NB (0.8 mm/m), which expand moderately. High expansion > 1.0 mm/m is shown by BP, LOS, BS and CV, with maximum values of up to 2.5 mm/m (BS). HR is a special case, that shows slight contraction of − 0.1 mm/m. This phenomenon was also observed on one SMA sample. Already Snethlage and Wendler (1997) observed a contractional behavior upon moisture absorption and an extension upon drying on a clay-rich sandstone, that was pretreated with a salt solution (NaCl). Steiger et al. (2011) explain this behavior with the influence of salt crystallization-dissolution on the process of hydric expansion. They argue that if salt crystallizes from saturated solutions in the pore space during

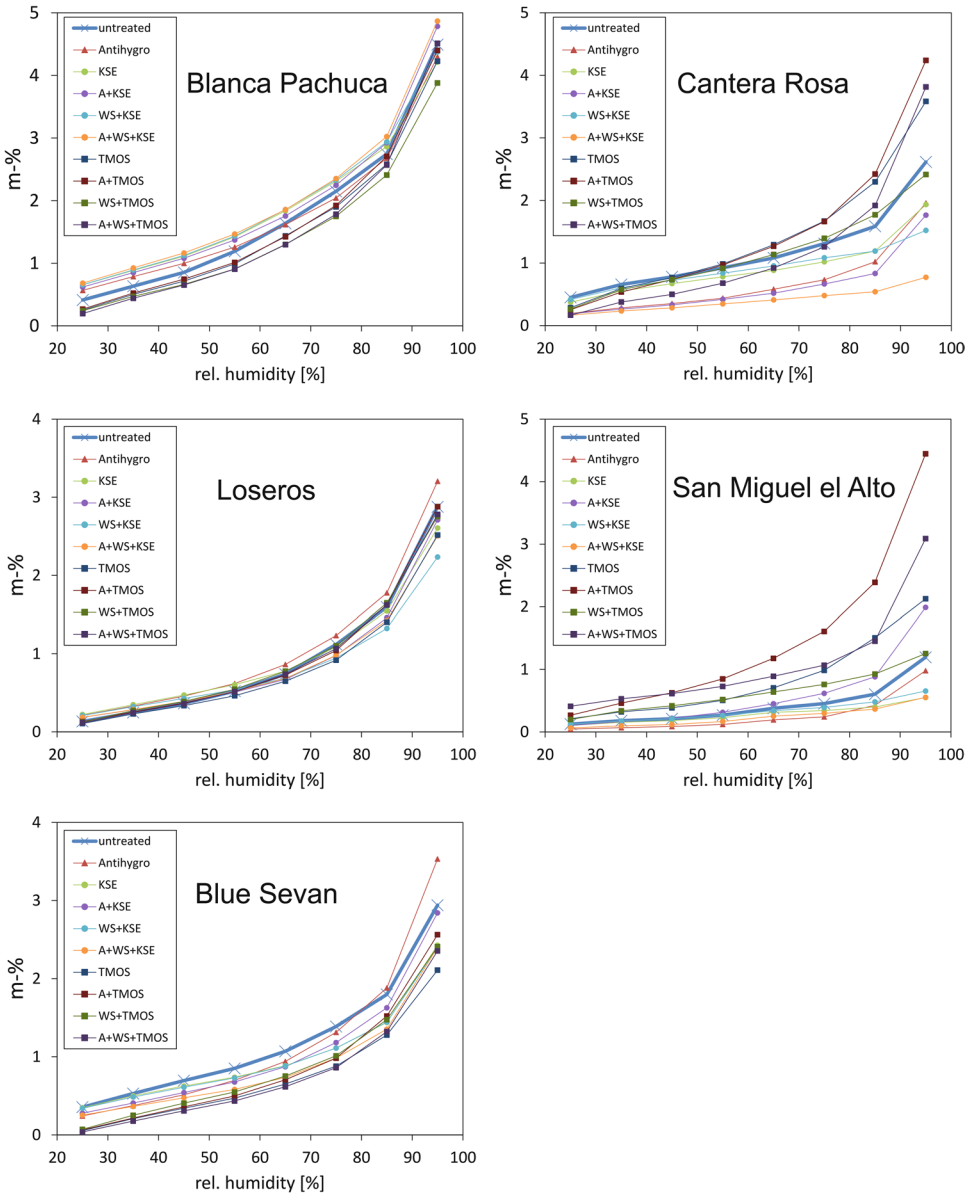

Fig. 12 Modification of the adsorption isotherm of BP, CR, LOS, SMA and BS due to the consolidation treatments

drying periods, it creates a crystallization pressure, inducing an expansion in the stone fabric. The dissolution of these salt crystals will consequently lead to a relaxation and contraction. Thus, in dry conditions, a salt enriched sample will already be expanded and may show a contractional behavior upon wetting, because the salt crystals will dissolve. The excess of salts in the pore space of both HR and SMA after the treatment with Antihygro (see surface efflorescence in Fig. 6) may cause this exact phenomenon. The salts were, however, not further analyzed in this study.

According to Snethlage and Pfanner (2020) an increase of the expansional behavior due to the conservational treatment should be avoided under any circumstances. The application of TEOS only, however, lead to a higher hydric expansion of the tuffs. This effect was even increased with a primer component (WS) pretreatment (Fig. 14). The hydric expansion of CR, for example, was more than tripled, up to 0.8 mm/m. The application of an anti-swelling agent (A), on the other hand, reduced the hydric expansion in nearly every case. Even in combination with TEOS (or primer component and TEOS) the hydric expansion of the tuffs could be reduced or did not increase. In BP and NB, as well as CV in combination A + WS + KSE, the anti-swelling agent could not compensate the increased swelling due to the consolidation. Another observation after the treatments is an often reduced anisotropic behavior in hydric expansion of the investigated rocks.

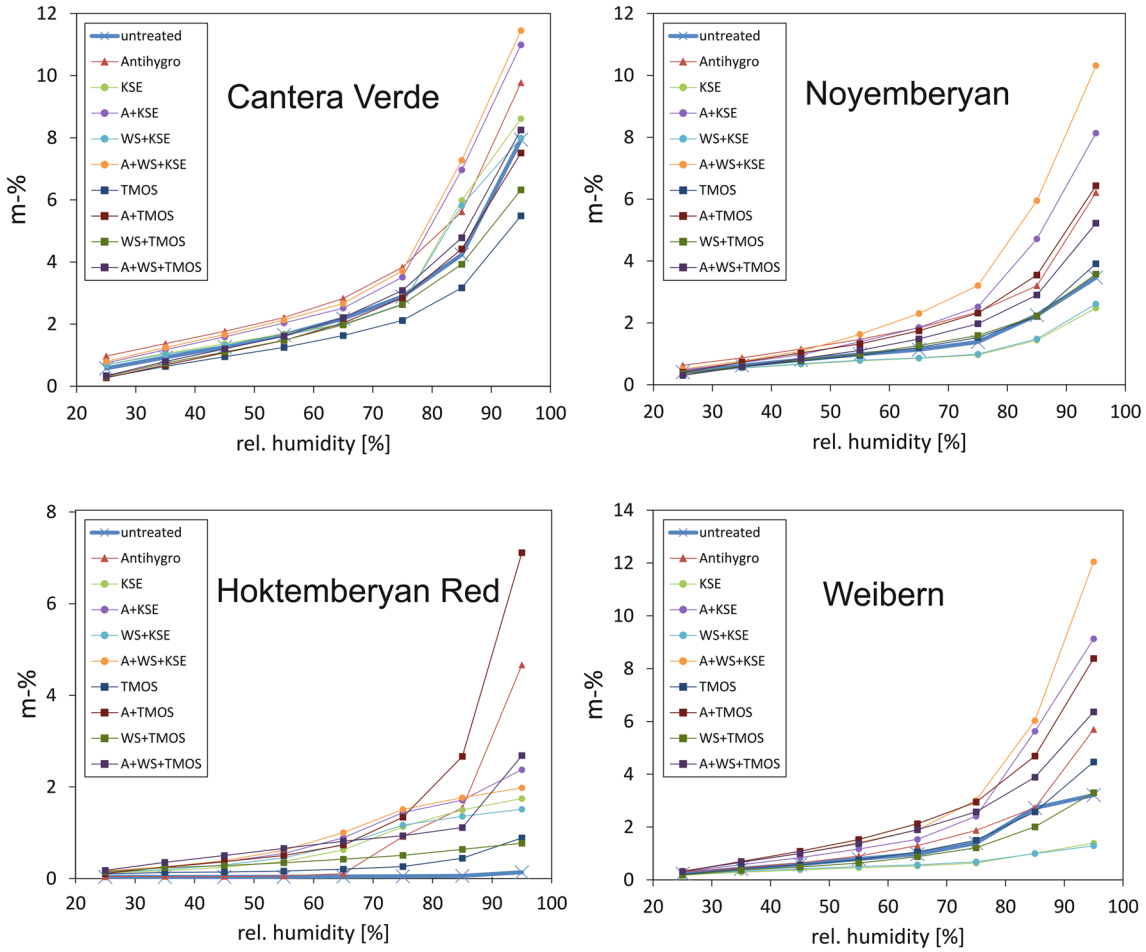

Fig. 13 Modification of the adsorption isotherm of CV, NB, HR and WB due to the consolidation treatments

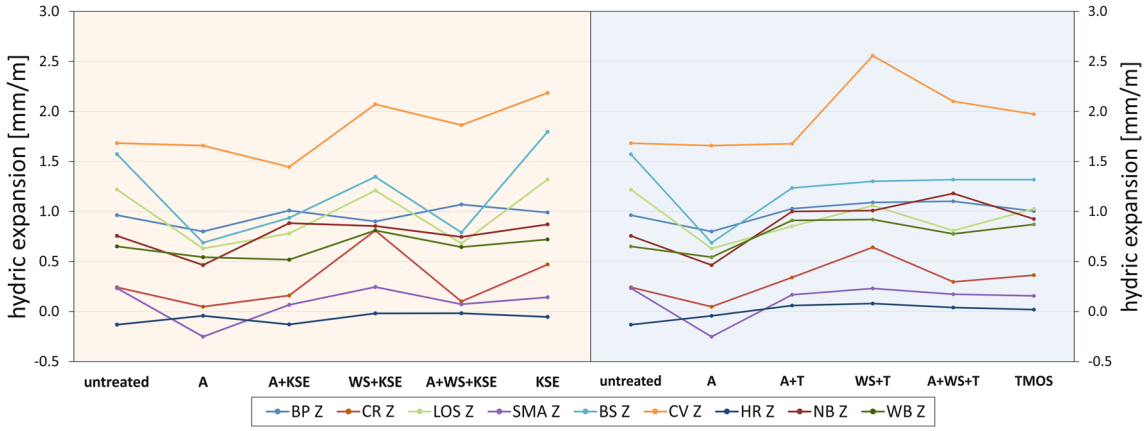

Fig. 14 Modification of the hydric expansion in Z direction due to the consolidation treatments. Left) TEOS, right) TMOS

The consolidation with TMOS produced quite similar trends for the different combinational treatments. However, the increase of hydric expansion is often markedly lower. Exceptions are NB and WB, which show a slightly stronger increase of expansion compared to consolidation with TEOS.

Thermal and thermo-hydric expansion

The enormous mineralogical variety and broad range of textural and fabric variability has a great impact on the expansional behavior of tuffs, since the thermal expansion coefficient α is a result of the expansion of the individual minerals present in the rock. This makes the prediction of the thermal expansional behavior of tuffs very difficult. López-Doncel et al. (2018) give an overview of these problematics and observed some trends like increased thermal expansion of acid, crystal-rich and more homogeneous tuffs. In general, α is only considered with regard to the thermal expansion under dry conditions. In this section it will, however, also be used as an expression of the expansional behavior under thermo-hydric (wet) conditions.

Regarding the thermal (dry) and thermo-hydric (wet) expansion, the tuffs of this study show coefficients of linear thermal expansion (α) between 6.8 and 13.4×10^{-6} K^{-1} under dry conditions, that increase significantly under wet conditions ($7.2–50.7 \times 10^{-6}$ K^{-1}) (Table 3). In doing so, the highest values often coincide with the tuffs that contain formidable amounts of swelling clays and/or zeolites and simultaneously showing the highest hydric expansion values (compare Tables 2 and 3). Under wet conditions the strong influence of hydric expansion has to be considered, since most minerals would not be able to produce such high α-values on their own (compare α for different minerals in Steiger et al. (2011)).

The change of expansional behavior due to thermal stress (dry) for most consolidated tuffs is within the framework of ± 20% with regard to their untreated state. CV is an exception, showing an extreme increase of its' α value after any combinational treatment with both TEOS and TMOS, when tested under dry conditions (Fig. 15). Under wet conditions, the thermo-hydric expansion of CV is reduced strongly after both TEOS and TMOS treatment, especially when consolidated in combination with the anti-swelling agent. The sole application of TEOS tends to slightly increase the thermal and thermo-hydric expansion of the tuffs. On the contrary, the sole consolidation with TMOS, and most combinational

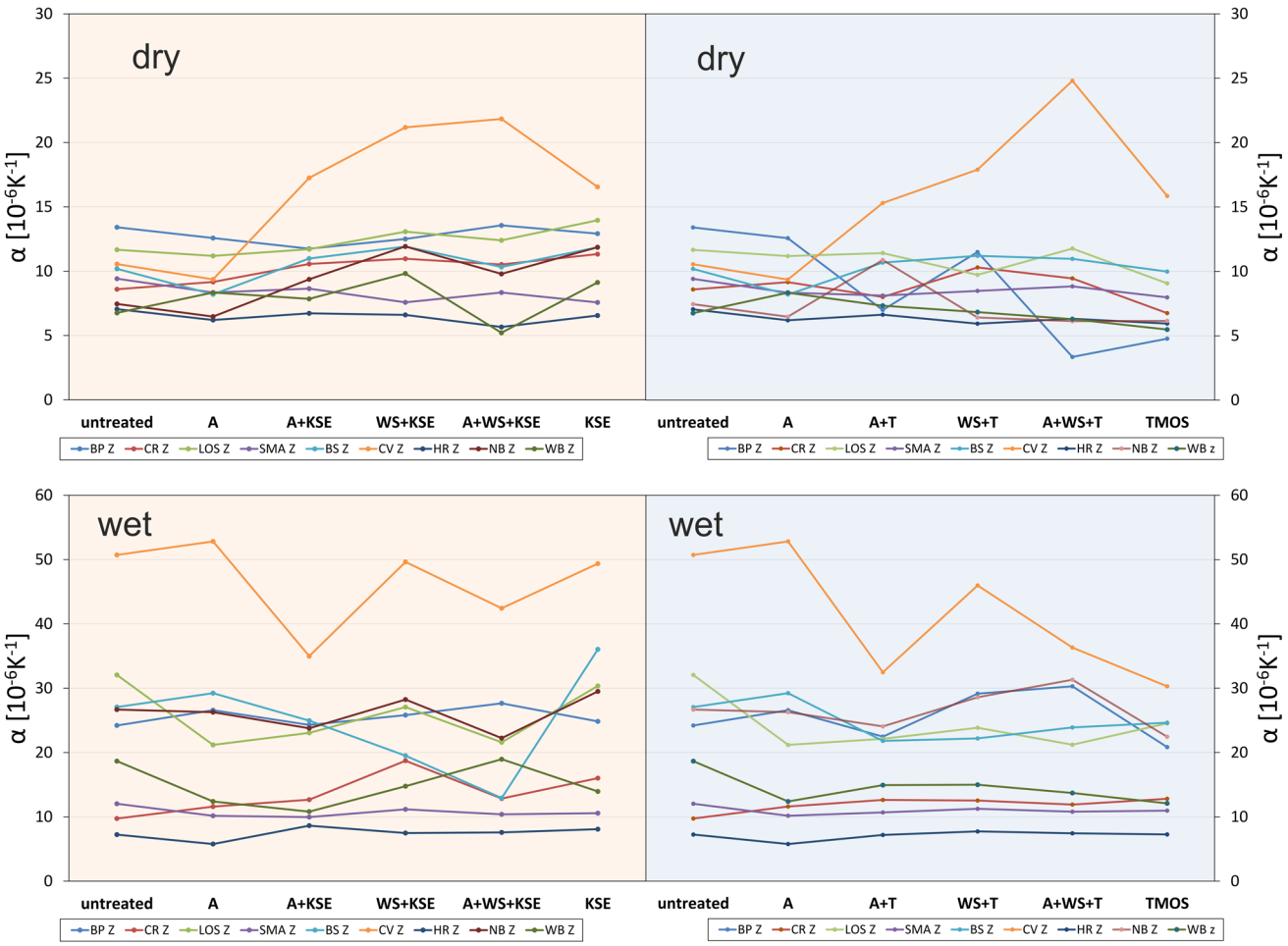

Fig. 15 Modification of the thermal expansion coefficient α under dry and wet conditions in Z direction due to the consolidation treatments. Left) TEOS, right) TMOS

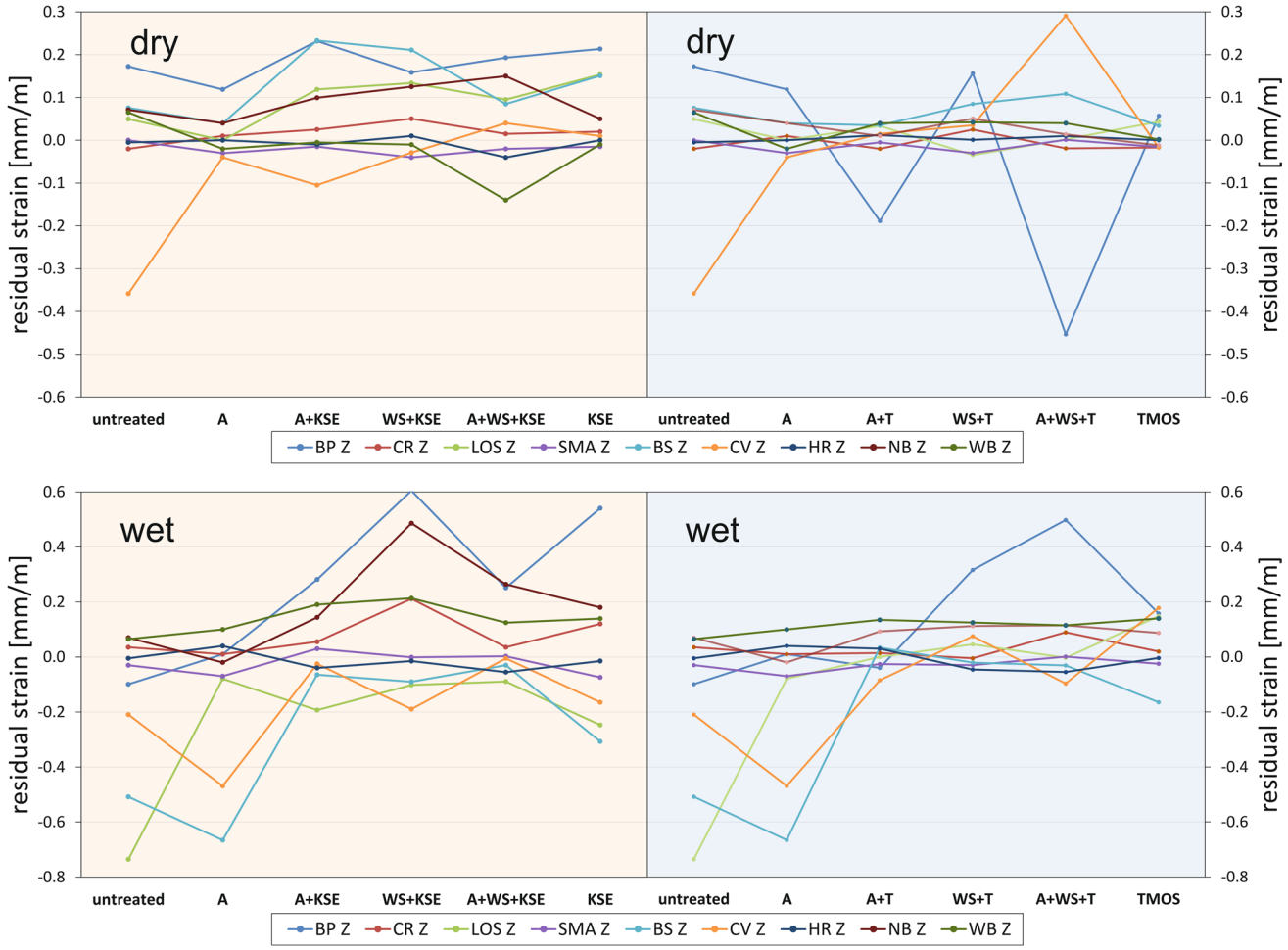

Fig. 16 Modification of the residual strain ε after thermal (dry) and thermo-hydric (wet) expansion in *Z*-direction due to the consolidation treatments. Left) TEOS, right) TMOS

treatments with TMOS, lead to a decreasing thermal and thermo-hydric expansion. Modifications are typically stronger for low porous tuffs. The expansional behavior of SMA and HR was barely affected by any treatment, neither under dry nor wet conditions.

Despite their partly high α-values, only BP and CV show considerable residual strain (ε) after thermal treatment under dry conditions (Fig. 16). In doing so, BP shows positive residual strain around 0.17 mm/m, while CV shows a strong negative residual strain of up to 0.54 mm/m. Under wet conditions both samples show reduced negative residual strain of up to 0.10 mm/m (BP) and 0.25 mm/m (CV), respectively. LOS and BS develop highly negative residual strains in Z direction (perpendicular to the bedding) under wet conditions of 0.74 mm/m and 0.51 mm/m, respectively.

While SMA, HR and for the most part CR do not experience considerable changes in their residual strain after thermal and thermo-hydric stress, WB, NB and BP consolidated with TEOS show significant higher residual strains after thermo-hydric stress. Furthermore, after thermal stress under dry conditions, NB, LOS and BS consolidated with TEOS in any combinational treatment show moderate increase of the residual strain. The strongest increase is usually caused by the application of TEOS (KSE) only or in combination with tartaric acid (WS + KSE).

Most of the tuffs consolidated with TMOS do not show an increase of their residual strain. On the contrary, the highly negative residual strains of LOS, BS and CV under wet conditions were drastically reduced (Fig. 16). On BP, however, the combination of TMOS with an anti-swelling agent or tartaric acid lead to highly negative residual strain (up to 0.45 mm/m) under dry conditions (A + T/A + WS + T) and highly positive residual strain (up to 0.50 mm/m) under wet conditions (WS + T/A + WS + T/TMOS).

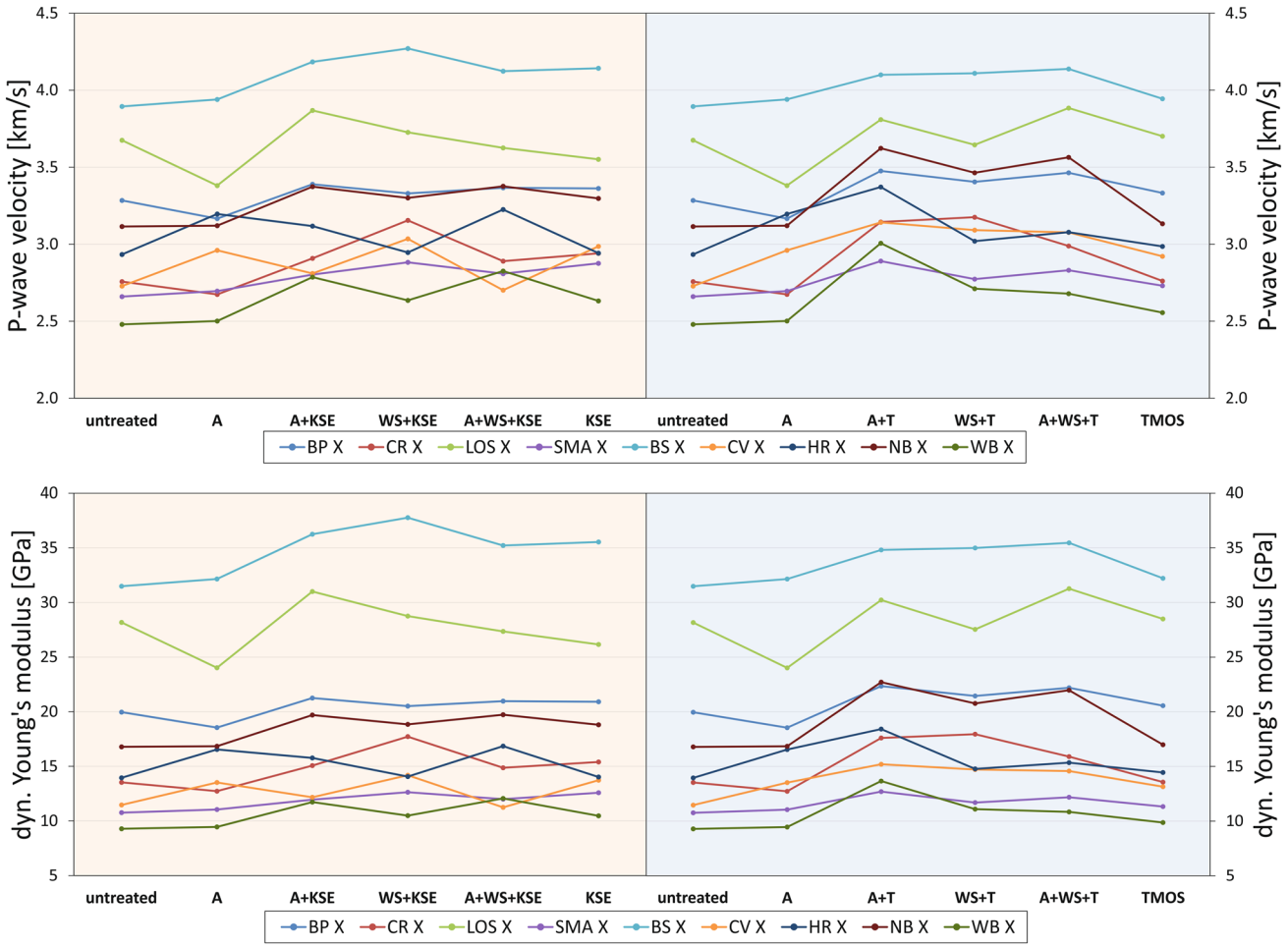

Fig. 17 Modification of the ultrasonic (P-wave) velocity and dynamic modulus of elasticity (Young's Modulus) due to the consolidation treatments. Left) TEOS, right) TMOS

Modification of the ultrasonic velocity and dynamic modulus of elasticity

In general, only a direct assessment of the strength parameters via compressive, tensile or flexural strength test can verify the true strength gain or loss after a consolidation treatment. The strength of rock material is, however, proportional to the dynamic modulus of elasticity (Young's Modulus), which can be determined from ultrasonic measurements (Siegesmund and Dürrast 2011). Pötzl et al. (2021) found strong correlation of the ultrasonic velocity with both compressive and tensile strength on over 200 tuffs. As the correlations are rock-dependent they should be specified for the rocks under consideration in further research. The results for the ultrasonic velocities and dynamic Young's Moduli parallel to the bedding (*X* direction) are displayed in Fig. 17. The ultrasonic velocities of the untreated tuffs range between 2.5 and 3.9 km/s, whereby the highest velocities are shown by the low porous tuffs BP, LOS and BS and typically parallel to the bedding.

All tuffs experience an increase of the ultrasonic velocity after consolidation treatment. Except for SMA and BS, the increase is higher after the application of TMOS, especially in combination with the Antihygro (A + T/A + WS + T). Combinational treatment of TEOS with the Antihygro (A + KSE/A + WS + KSE) produced the strongest increase for BP, LOS, HR, NB and WB, while the combination with the tartaric acid (WS + KSE) led to the strongest increase of ultrasonic velocity for BS, CR, CV and SMA (Fig. 17).

Except for WB, all tuffs show a more or less pronounced directional dependence on their ultrasonic velocities, with higher velocities in *X* direction (Table 3). After the consolidation the anisotropic behavior remains unchanged for most tuffs. In WB and CV the application of both TEOS and TMOS lead to increased directional dependence, while in LOS the treatment with TMOS and in HR the treatment with TEOS slightly decreased the anisotropic effects.

The dynamic Young's Moduli naturally show trends similar to the ones that can be observed for the ultrasonic velocities, pointing to a general increase of strength by all consolidation treatments (Fig. 17). The increase in strength is more pronounced in the highly porous tuffs and the highest increase in strength for most samples can be observed after treatment with Antihygro and TMOS (A + T). Other than that, when TEOS is applied, the strongest increase is observed in combination with the tartaric acid (WS + KSE/A + WS + KSE). In their catalog of requirements Snethlage and Pfanner (2020) consider an increase of the dynamic Young's Moduli of more than 1.5 times the value of the unweathered stone as critical. An overstrengthening of the consolidated zone should be prevented by all means, since it may induce considerable stress at the interface of treated and untreated material. This limit is exceeded only once for HR, by the treatment TMOS in combination with Antihygro (A + T).

A reduction of strength is shown by CV when treated with TEOS in combination with Antihygro (A + KSE). With additional tartaric acid (A + WS + KSE) the strength reduction is intensified up to − 20%. Apart from that, a strength reduction of up to − 15% can be observed for BP, CR and LOS due to the treatment only with Antihygro.

Discussion

The treatment of nine different tuffs with a commercially available stone consolidant (TEOS) and the utilization of a neat product with smaller molecule size (TMOS), in different combinations of applications with a primer component and a swelling reducer, generated clear but ambivalent results:

TEOS

The consolidation with TEOS led to a significant reduction of the porosity, fraction of micropores, total and capillary water absorption. These modifications of the stone properties are expected to lead to a higher weathering resistance. Increasing water vapor diffusion resistance, however, can possibly lead to drying problems of the stone and in extreme cases to the creation of a diffusion barrier that can trap water inside the stone, which is subsequently involved in e.g., crystallization-dissolving processes. In this regard, especially the low to moderate porous tuffs show an alarming development.

Regarding the moisture expansion, slight increases up to a partial tripling of the hydric expansion could be observed. This is obviously an undesired side effect and reduces the weathering resistance of the tuffs. However, this negative side effect could be counteracted by pretreating the sample with an anti-swelling agent. Therefore, given a pretreatment with an anti-swelling agent, an application of TEOS on the investigated tuffs is expected to increase their weathering resistance. The same applies with regard to the thermal expansion. The consolidation shows limited effects on the thermal expansion behavior of most tuffs. The clay-rich, low to moderate porous tuffs BS, NB and LOS show moderately increased residual strain. Under wet conditions, the alarming increase of residual strain in the zeolite-rich samples BP, NB and WB has to be evaluated negatively. The clay and zeolite-rich CV experienced significantly stronger expansion, its' residual strain, however, could be reduced by the TEOS treatment.

The application of tartaric acid as a primer component strikingly enhances the effect of the consolidation with TEOS. Especially the modifications on water transport and retention are strongly increased in comparison to an application of consolidant only. As mentioned above, this is likely because residual tartaric acid would promote hydrolysis and reduce hydrophobicity, which is usually caused by the consolidant. It should be noted, however, that a pretreatment with the primer component always enhances both positive and negative effects of the consolidant, e.g., further reduction of the porosity or increase of hydric expansion, respectively. A very positive effect observed during the consolidation treatment itself, was a strongly accelerated absorption of the consolidant after the pretreatment with the primer component (see also Fig. 4).

The lack of significant strength increase can be evaluated as a positive outcome, because it reveals that the consolidation did not result in an over-strengthening of the material, since in this study unweathered material was treated. Thus, no major stress disparities between treated and untreated areas of the tuffs are expected. In addition, it allows for a repeated treatment to increase the consolidation effects. As mentioned in the previous section, in the future direct measurements of the compressive, tensile or flexural strength have to verify the findings on rock strength modifications that were derived by ultrasonic measurements in this study.

Figure 18 displays precipitated TEOS and TMOS in the pore space of a low porous (BP) and a highly porous (SMA) tuff. A significant coating of the pore space can be observed and the silica gel shows typical dry cracks that explain the development of smaller micropores registered in the pore radii distribution of the tuffs (Tab.E1–9 in the ESM). The initial bonding to the substrate appears to be good.

TMOS

The consolidation with TMOS generated similar results regarding the reduction of the porosity, total and capillary water absorption, as well as an increase of the water vapor

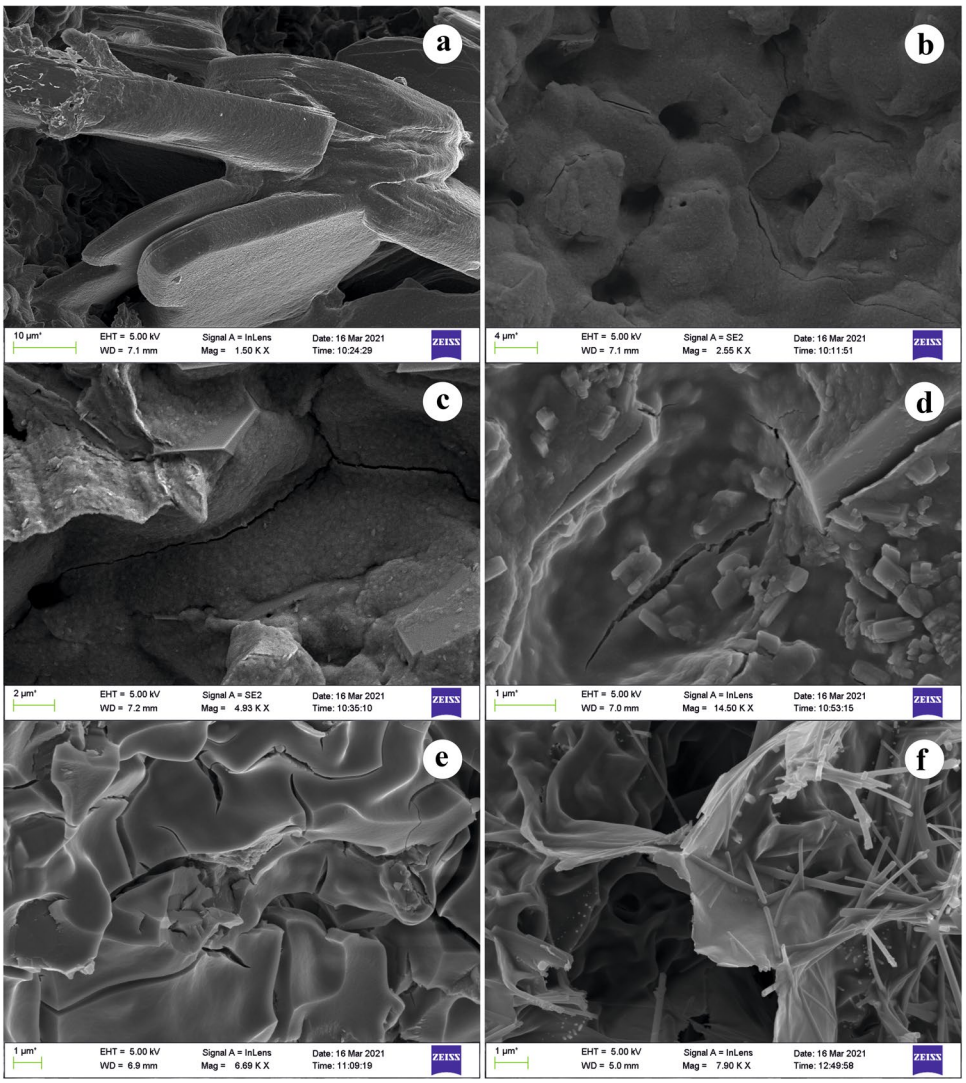

Fig. 18 SEM photomicrographs of the fully cured silica gel produced by either TEOS or TMOS treatment. **a** Individual crystals covered with silica gel from TEOS treatment in the tuff SMA. **b** The silica gel, with typical dry cracks, covers the matrix and leads to a reduction of pore space and narrowing of pathways in SMA treated with TEOS. **c** Feldspar crystals barely stand out of the cover of silica gel in SMA. The silica gel formed by TEOS treatment has a rather rough surface. **d** + **e** The silica gel formed by TMOS treatment of the same tuff (SMA) is thicker, has a smoother surface and more pronounced dry cracks. **f** In the rather low porous tuff BP, the silica gel formed by TMOS treatment works like a glue and sticks together the individual mordenite needles

diffusion and hydric expansion. However, compared to the treatments with TEOS, the changes are usually less pronounced, especially in high porous tuffs, but more intense in low porous tuffs with an abundance in zeolites and swelling clays.

In contrast to TEOS, TMOS significantly increased the fraction of micropores and therefore the specific surface area, especially in the low porous tuffs. The changes towards a bimodal pore character with a high share of micropores are alarming, since bimodal pore size distributions have shown to increase the weathering susceptibility of tuffs (Wedekind et al. 2013; López-Doncel et al. 2016; Pötzl et al. 2018a, b). However, the tuffs do not show a resulting increase in hydric, thermal or thermo-hydric expansion. In fact, the expansional behavior of tuffs treated with TMOS is less negatively influenced than with TEOS. Thermal expansion is even decreased (with exception of CV). The clay and zeolite-rich, low porous BP develops residual strain after thermal stress, which has to be evaluated critically. Consolidation with TMOS led to a slightly stronger strength increase than TEOS, but is still within the acceptable range of deviation after Snethlage and Pfanner (2020). If the modified pore character of the tuffs might negatively influence their durability should be further explored using salt bursting tests. An increased fraction of micropores, for example, may potentially retain aqueous (salt saturated) solutions for a longer period of time that lead to a delayed drying behavior of the tuff and an extended supply of salt solution for the crystallization of halides in adjacent pores.

Unlike for TEOS, the pretreatment with tartaric acid did not significantly increase the effect of TMOS. On the contrary, in many cases the application of sole TMOS led to more intense modifications. The most significant enhancement of the consolidation effects of TMOS were reached by the pretreatment with the anti-swelling agent. The Antihygro itself is basic (pH 8.5) and may have a catalytic impact on the consolidation process, since we know that the hydrolysis

reaction can be enhanced by either acidic or alkaline catalysis (Snethlage and Sterflinger 2011).

The SEM photomicrographs in Fig. 18 reveal that the silica gel formed by TMOS is generally thicker than the gel formed by TEOS and shows a smoother surface. Dry cracks are more abundant and create a secondary porosity in the submicrometer range, likely in the nanometer range. In general, TMOS treated samples show a significant higher amount of silica gel in their pore space than samples treated with TEOS.

General remarks

The petrophysical properties of the tuffs were partly modified to a point, such that they did not meet the requirements of the quality catalog of Snethlage and Pfanner (2020) anymore. Especially the water vapor diffusion resistance was often increased by more than 50%, which bears the risk of the creation of a diffusion barrier and potentially trapped water may induce freeze–thaw attack upon temperature changes or interact with salts and clay minerals. The reduction in strength through water absorption was successfully identified in the literature (Hirschwald 1908; Vásárhelyi 2002; Török et al. 2004; Morales Demarco et al. 2007; Siedel 2010; Çelik and Ergül 2015; Hashiba and Fukui 2015; Pötzl et al. 2018a) and even small amounts of moisture may induce significant strength reduction (Yasar 2020).

A darkening of the stone is an undesired side effect, that was primarily observed on high porous tuffs by the application of TEOS and on low porous tuffs by the application of TMOS (Fig. 5). In addition, the application of TMOS on zeolite rich tuffs pretreated with Antihygro showed a glossy appearance. A glossy appearance is to be avoided by any means and usually indicates that the moisture content during the application was too high, so that the silica gel already precipitates at the surface of the specimen (Snethlage and Sterflinger 2011). In this case, however, the accelerated precipitation at the surface of the tuff was likely caused by the pH of the Antihygro (pH 8.5) as higher pHs promote rapid condensation and gelation.

Conclusions

The consolidation of volcanic tuffs is a challenging topic. Many products that proved to produce satisfying results for other types of porous stones fail in the application on tuff. Essential problems are the water retention of some tuffs and small nanopores that aggravate the absorption of the consolidant. The main goals of this study were:

1. to investigate the general suitability and influence of TEOS and TMOS on the petrophysical properties and material behavior of different types of tuffs.
2. to determine the effects of a primer component (tartaric acid) and anti-swelling agent (Antihygro) on consolidation treatments of different volcanic tuffs.
3. to investigate if TMOS, due to the smaller molecule size of its monomers, is being absorbed more effectively than common TEOS products.

The evaluation of the petrophysical properties before and after the consolidation with TEOS and TMOS identified varying efficiency and suitability for different types of tuff. Some findings of this laboratory investigation may also prove useful for the practical in-situ application:

- The effect of the consolidation with both TEOS and TMOS is generally higher on clay and zeolite-rich, low porous tuffs. Comparing the effectiveness of both consolidants, TEOS appears to induce modifications of the petrophysical properties more effectively on highly porous rock, while TMOS showed to be more effective on low porous tuffs.
- The pretreatment with tartaric acid significantly enhanced the effects of TEOS, both beneficial and unfavorable. In this regard a benefit-risk assessment is crucial before the practical application. For example, does an increased strengthening effect outweigh a potential increase in expansional behavior? An enhancing effect of the primer to the degree observed for TEOS cannot be noted for TMOS.
- In combination with TEOS and TMOS, the anti-swelling agent significantly counteracted the increasing hydric expansion, originating from the consolidants.
- The anti-swelling agent showed almost exclusively positive modifications of the stone properties and may be applied in most cases without expecting negative side effects if the tuffs are rich in swelling clays. The highly porous tuffs containing no (HR, WB) or barely (SMA) swelling clay minerals, did show salt efflorescence after the application of the anti-swelling agent which itself is a salt(1,4-diaminobutane dihydrochloride). It can be assumed that the Antihygro is causing the excess of salt in these tuffs, since the specimens of the same lithology that were not treated with Antihygro did not show any efflorescence. The two molecules of dihydrochloride in diaminobutane dihydrochloride dissociate in aqueous solution and produce two Cl^- that may react with cations of alkaline or alkaline earth metals, namely Na, K, Mg and Ca, and form corresponding halides. The most natural halide to crystallize under ambient conditions (20 °C, RH < 70%) is sodium chloride or halite. SMA and HR experienced an increasing contractional behavior upon wetting after the treatment with Antihygro. Steiger et al. (2011) state that such contractional behavior upon wetting, points to the fact that salt crystals, build in the pore

space from the excess salt during dry periods, induce constant crystallization pressure to the stone fabric. The stone fabric that is therefore under expansion during dry conditions, will contract upon wetting and subsequent dissolution of the salt crystals. In the case of recurring wet-dry cycles, the salt will induce progressive damage to the stones, which underlines the importance of a desalination prior to the consolidation. Considering the relatively low hydric expansion values of untreated HR, SMA and WB, the application of an anti-swelling agent does not seem to benefit its petrophysical modification enough to outweigh a slight decrease of hydric expansion. We conclude, that it seems only recommendable to apply Antihygro on tuffs when an inhibition of the hydric expansion is truly needed and never as a prophylactic measure, as there is a risk of excessive salt efflorescence. In any case, if salt efflorescence is visible, the stone should be desalinated prior to the consolidation treatment.

- Low porous tuffs absorbed TMOS significantly stronger than TEOS (Fig. 4), with drawbacks only in exceptional cases. The partly extreme changes of the pore size character due to the shift of pore classes towards single digit nanopores suggest that the TMOS either entered and precipitated inside the smaller micropores (clogging of pore throats). Or the silica gel itself caused an extreme amount of secondary micropores, for example due to dry cracks as a result of the polycondensation. SEM photomicrographs of TMOS treated tuff revealed, that both is the case (Fig. 18).

In summary, this study provides a variety of data that indicates, that TMOS may be a suitable candidate to overcome the bottlenecks in the pore space of tuffs, which limit the consolidation success of current products. Note that the study was conducted under controlled laboratory conditions on fresh quarry material. The samples were first preconditioned and then fully saturated during the consolidation, to guarantee the same conditions for every stone and identify general suitability. On-site application would neither allow such controlled preconditioning of the stone (building elements), nor a full saturation with the consolidant. The results of the treatment of unweathered material are moreover not transferable one-to-one to weathered material, which may show entirely altered pore space, for example due to the creation of cracks. The next step should be the investigation of the depth profile of suitable candidates and the characterization of their capillary absorption of the consolidants. Regarding the strength increase due to a consolidation measure, Doehne and Price (2010) refer to the results of Félix (1996) and Scherer and Jiménez-González (2008), who observed a loss of the initially increased strength in consolidated clay-bearing stones, after only three to ten dry/wet cycles. Subsequent steps should be the durability testing of the consolidation in long term experiments and a potential application on on-site test fields. Our investigation demonstrates that supplementary treatments of both TEOS and TMOS could be also conceivable. Once more it has to be highlighted that prior to every practical on-site application, extensive preliminary investigations have to be undertaken, to maximize the desired consolidation effect and minimize the risk of causing irreversible damage.

Supplementary Information The online version contains supplementary material available at https://doi.org/10.1007/s12665-021-10066-1.

Acknowledgements We are grateful to R. Dohrmann, K. Wemmer, A.Kück, M. Rittmeier, K. Ufer, N. Schleuning, A. Marx and M. Sitnikova for their laboratory support and help with the mineral analyses. We thank T. Licha, J. Menningen and M. Hueck for many helpful comments and C. Gross for the English corrections. We are especially grateful to V. Safaryan for the help with the sampling and sample transfer to Germany. This work was supported by the German Research Foundation (Si-438/52-1) and the Volkswagen Foundation (AZ93919). C. Pötzl gratefully acknowledges the financial support by the German Federal Environmental Foundation (AZ20017/481), the German Academic Exchange Service (ID 57212311) and the Georg-August-University School of Science (RTG2019). Finally, we want to thank the two anonymous reviewers for many helpful suggestions that greatly improved the manuscript.

Author contributions CP: conceptualization, methodology, analysis, investigation, writing, editing, funding acquisition. SR: analysis, investigation, editing. EW: conceptualization, methodology, editing. SS: supervision, project administration, funding acquisition.

Funding Open Access funding enabled and organized by Projekt DEAL. This work was supported by the German Research Foundation (Si-438/52-1) and the Volkswagen Foundation (AZ93919). C. Pötzl gratefully acknowledges the financial support by the German Federal Environmental Foundation (AZ20017/481), the German Academic Exchange Service (ID 57212311) and the Georg-August-University School of Science (RTG2019).

Availability of data and materials The datasets used and/or analyzed during the current study are available from the corresponding author on reasonable request. Additional electronic supplementary material is accompanied by this paper.

Declarations

Conflict of interest The authors declare that there are no conflicts of interest.

Ethics approval The author declare that all principles of ethical and professional conduct have been followed.

Consent to participate All authors agreed to participate.

Consent for publication All authors consent for publication.

References

Auras M, Steindlberger E (2005) Verwitterung und Festigung vulkanischer Tuffe. In: Zeitschrift der Deutschen Gesellschaft für Geowissenschaften, pp 167–175

Çelik MY, Ergül A (2015) The influence of the water saturation on the strength of volcanic tuffs used as building stones. Environ Earth Sci 74(4):3223–3239

de Pablo-Galán L (1986) Geochemical trends in the alteration of Miocene vitric tuffs to economic zeolite deposits, Oaxaca, Mexico. Appl Geochem 1(2):273–285

Doehne E, Price CA (2010) Stone conservation. An overview of current research. An overview of Current Research. Getty Conservation Institute (ed), Canada

Dohrmann R, Kaufhold S (2009) Three new, quick CEC methods for determining the amounts of exchangeable calcium cations in calcareous clays. Clays Clay Miner 57(3):338–352

Egloffstein P (1998) Vulkanische Tuffsteine als Werksteine an historischen Bauwerken in Ungarn und Deutschland–Verwitterungsverhalten und Konservierungskonzepte

Félix C (1996) Peut-on consolider les grès tendres du Plateau suisse avec le silicate d'éthyle?

Fisher RV (1966) Rocks composed of volcanic fragments and their classification. Earth Sci Rev 1(4):287–298

Hashiba K, Fukui K (2015) Effect of water on the deformation and failure of rock in uniaxial tension. Rock Mech Rock Eng 48(5):1751–1761

Hirschwald J (1912) Handbuch der bautechnischen Gesteinsprüfung für Beamte der Materialprüfungsanstalten und Baubehörden, Steinbruchingenieure, Architekten und Bauingenieure: sowie für Studierende der technischen Hochschulen, Vol. 2. Gebrüder Borntraeger

Hirschwald J (1908) Die Prüfung der natürlichen Bausteine auf ihre Wetterbeständigkeit. W. Ernst & Sohn

Korkuna O, Leboda R, Skubiszewska-Zie BJ, Vrublevs'ka T, Gun'ko VM, Ryczkowski J (2006) Structural and physicochemical properties of natural zeolites: clinoptilolite and mordenite. Microporous Mesoporous Materi 87(3):243–254

López-Doncel R, Wedekind W, Leiser T, Molina-Maldonado S, Velasco-Sánchez A, Dohrmann R, Kral A, Wittenborn A, Aguillón-Robles A, Siegesmund S (2016) Salt bursting tests on volcanic tuff rocks from Mexico. Environ Earth Sci 75(3):212

López-Doncel R, Wedekind W, Aguillón-Robles A, Dohrmann R, Molina-Maldonado S, Leiser T, Wittenborn A, Siegesmund S (2018) Thermal expansion on volcanic tuff rocks used as building stones: examples from Mexico. Environ Earth Sci 77(9):338

Meier L, Kahr G (1999) Determination of the cation exchange capacity (CEC) of clay minerals using the complexes of copper (II) ion with triethylenetetramine and tetraethylenepentamine. Clays Clay Miner 47:386–388

Morales Demarco M, Jahns E, Rüdrich J, Oyhantcabal P, Siegesmund S (2007) The impact of partial water saturation on rock strength: an experimental study on sandstone. Zeitschrift Der Deutschen Gesellschaft Für Geowissenschaften 158(4):869–882

Nishiura T (1987) Laboratory test on the color change of stone by impregnation with silane

Poschlod K (1990) Das Wasser im Porenraum kristalliner Naturwerksteine und sein Einfluss auf die Verwitterung. Münchener Geowiss Abh B, vol 7

Pötzl C, Dohrmann R, Siegesmund S (2018a) Clay swelling mechanism in tuff stones: an example of the Hilbersdorf Tuff from Chemnitz, Germany. Environ Earth Sci 77(5):188

Pötzl C, Siegesmund S, Dohrmann R, Koning JM, Wedekind W (2018b) Deterioration of volcanic tuff rocks from Armenia. Constraints on salt crystallization and hydric expansion. Environ Earth Sci 77(19):660

Pötzl C, Siegesmund S, Lopez-Doncel R, Dohrmann R (2021) Key parameters of volcanic tuffs used as building stone: a statistical approach. Environ Earth Sci. https://doi.org/10.1007/s12665-021-10114-w

Pötzl C (2020) Volcanic tuffs as natural building stones. Mineralogy, technical properties, deterioration and conservation strategies. Dissertation, Georg-August-University, Göttingen

Rotare HM, Prenzlow CF (1967) Surface areas from mercury porosimetry measurements. J Phys Chem 71(8):2733–2736

Ruedrich J, Siegesmund S (2006) Fabric dependence of length change behaviour induced by ice crystallisation in the pore space of natural building stones. In Heritage, weathering & conservation: proceedings of the international conference on heritage, weathering and conservation. Taylor & Francis, p 497

Scherer G, Jiménez-González I (2008) Swelling clays and salt crystallization: The damage mechanisms and the role of consolidants

Scherer GW, Wheeler GS (2008) Silicate consolidants for stone. Key Eng Mater 391:1–25

Schmid R (1981) Descriptive nomenclature and classification of pyroclastic deposits and fragments: recommendations of the IUGS Subcommission on the Systematics of Igneous Rocks. Geology 9:41–43

Siedel H (2010) Historic building stones and flooding: changes of physical properties due to water saturation. J Perform Constr Facil 24(5):452–461

Siegesmund S, Dürrast H (2011) Physical and mechanical properties of rocks. In: Siegesmund S, Snethlage R (eds) Stone in architecture. Springer, pp 97–225

Snethlage R, Pfanner M (2020) Leitfaden Steinkonservierung: Planung von Untersuchungen und Maßnahmen zur Erhaltung von Denkmälern aus Naturstein, 5. vollständig überarbeitete und erweiterte Auflage

Snethlage R, Sterflinger K (2011) Stone conservation. In: Siegesmund S, Snethlage R (eds) Stone in architecture. Springer, pp 411–544

Snethlage R, Wendler E (1997) Moisture cycles and sandstone degradation. Environ Sci Res Rep ES 20:7–24

Steiger M, Charola AE, Sterflinger K (2011) Weathering and deterioration. In: Siegesmund S, Snethlage R (eds) Stone in architecture. Springer, pp 227–316

Steindlberger E (2020) Konservierung hessischer Tuffe und Schalsteine unter Langzeitbeobachtung. In: Institut für Steinkonservierung e.V. (ed) Konservierungsstrategien für Rhyolithtuffmauerwerk, Mainz, vol 60, pp 51–70

Steinhäußer U, Wendler E (2004) Conservation of limestone by surfactants and modified ethylsilicate

Stück H, Forgó LZ, Rüdrich J, Siegesmund S, Török A (2008) The behaviour of consolidated volcanic tuffs: weathering mechanisms under simulated laboratory conditions. Environ Geol 56(3–4):699–713

Török A, Gálos M, Kocsányi-Kopecskó K (2004) Experimental weathering of rhyolite tuff building stones and the effect of an organic polymer conserving agent. In: Stone decay: its causes and controls, pp 109–127

van Hees RPJ, Brendle S, Nijland TG, Haas G, Tolboom HJ (2003) Decay of Rhenish tuffs in Dutch monuments. Part 2: laboratory experiments as a basis for the choice of restoration stone. Heron 48(3):167–177

Vásárhelyi B (ed) (2002) Influence of the water saturation on the strength of volcanic tuffs. International Society for Rock Mechanics and Rock Engineering

Wedekind W, López-Doncel R, Dohrmann R, Kocher M, Siegesmund S (2013) Weathering of volcanic tuff rocks caused by moisture expansion. Environ Earth Sci 69(4):1203–1224

Wendler E, Klemm DD, Snethlage R (1991) Consolidation and Hydrophobic treatment of Natural Stone. In: Baker JM, Nixon PJ, Majumdar AJ, Davies H (eds) Durability of building materials and components: proceedings of the fifth international conference held in Brighton, UK, 7–9 November 1990, 1st edn, Spon, London, pp 203–212

Wendler E, Charola AE, Fitzner B (1996) Easter Island tuff: Laboratory studies for its consolidation. Berlin

Wendler E (2005) Probleme, Lösungsansätze und Erfolge bei der Konservierung von verwittertem Lapillituff. In: Evangelische Kirche von Kurhessen-Waldeck (ed) Konservierungskonzepte zum Erhalt von nordhessischem Tuffstein an historischen Bauwerken: Tagungsband; Abschlußbericht des DBU-Projektes "Innovative Konzepte zur Konservierung und zum Schutz umweltgeschädigter historischer Tuffsteinflächen am Beispiel von drei nordhessischen Kirchen ; Projekt Nr.: 18981–45, Kassel

Wendler E (2016) Engpässe im Porenraum: Kriterien für die gezielte Auswahl und Rezeptierung von Steinfestigern. In: IFS-Bericht, Institut für Steinkonservierung e.V. (ed) Unsere Denkmäler sind steinreich, vol 51, IFS, Mainz, pp 21–26

Wheeler GS, Newman R (1994) Analysis and treatment of a stone urn from the Imperial Hotel, Tokyo

Wheeler G, Mendez-Vivar J, Goins ES, Fleming SA, Brinker CJ (2000) Evaluation of alkoxysilane coupling agents in the consolidation of limestone. In: Fassina V (ed) Proc. of the 9th Int. Cong. on deterioration and conservation of stone. Elsevier Science, pp 541–545

Yasar S (2020) Long term wetting characteristics and saturation induced strength reduction of some igneous rocks. Environ Earth Sci 79(14):1–12